



저작자표시-비영리-변경금지 2.0 대한민국

이용자는 아래의 조건을 따르는 경우에 한하여 자유롭게

- 이 저작물을 복제, 배포, 전송, 전시, 공연 및 방송할 수 있습니다.

다음과 같은 조건을 따라야 합니다:



저작자표시. 귀하는 원저작자를 표시하여야 합니다.



비영리. 귀하는 이 저작물을 영리 목적으로 이용할 수 없습니다.



변경금지. 귀하는 이 저작물을 개작, 변형 또는 가공할 수 없습니다.

- 귀하는, 이 저작물의 재이용이나 배포의 경우, 이 저작물에 적용된 이용허락조건을 명확하게 나타내어야 합니다.
- 저작권자로부터 별도의 허가를 받으면 이러한 조건들은 적용되지 않습니다.

저작권법에 따른 이용자의 권리는 위의 내용에 의하여 영향을 받지 않습니다.

이것은 [이용허락규약\(Legal Code\)](#)을 이해하기 쉽게 요약한 것입니다.

[Disclaimer](#)

2024년 2월
박사학위 논문

Characterization of PI3Ks, DydA and Shaker-like Potassium Channel Proteins in Cell Migration

조선대학교 대학원

글로벌바이오융합학과

김 원 범

Characterization of PI3Ks, DydA and Shaker-like Potassium Channel Proteins in Cell Migration

세포이동에서 PI3Ks, DydA 및 Shaker-like 칼륨
채널 단백질의 역할 규명

2024 년 2 월 23 일

조선대학교 대학원

글로벌바이오융합학과

김 원 범

Characterization of PI3Ks, DydA and Shaker-like Potassium Channel Proteins in Cell Migration

지도교수 전택중

이 논문을 이학박사학위 신청 논문으로 제출함

2023년 10월

조선대학교 대학원

글로벌바이오융합학과

김원범

김원범의 박사학위논문을 인준함

위원장 조 광 원 (인)

위 원 전 택 중 (인)

위 원 이 준 식 (인)

위 원 이 한 용 (인)

위 원 성 하 철 (인)

2024년 1월

조선대학교 대학교

CONTENTS

LIST OF FIGURES..... iv

ABBREVIATIONS..... vi

ABSTRACT..... vii

초록..... x

GENERAL INTRODUCTION..... 1

**PART I. Phosphatidylinositol 3-kinases play a suppressive role
 in cell motility of vegetative *Dictyostelium* cells**

I. INTRODUCTION..... 13

II. MATERIALS AND METHODS..... 15

II-1. Strains and cell cultures 15

II-2. Electrotaxis and quantitative..... 15

II-3. Random migration 16

II-4. Statistics 16

III. RESULTS..... 17

III-1. Electrotaxis of wild-type cells in the presence of LY294002..... 17

III-2. Electrotaxis of *pi3k1/2* null cells in the presence of LY294002..... 22

III-3. Random motility based on cell state in the presence of LY294002...25

IV. DISCUSSION.....29

PART II. Dynamic subcellular localization of DydA in

Dictyostelium cells

I. INTRODUCTION.....32

II. MATERIALS AND METHODS34

 II-1. Strains and plasmids34

 II-2. Chemotaxis and image acquisition34

 II-3. Quantitative analysis of membranes localization.....35

III. RESULTS36

 III-1. Domain structure of DydA and localization of DydA36

 III-2. Characterization of the domains of DydA for localization38

 III-3. Actin foci localization of DydA.....41

 III-4. Colocalization of GFP-PRM and RFP-coronin43

IV. DISCUSSION46

PART III. Role of Shaker-like potassium channels in cell

migration in Dictyostelium

I. INTRODUCTION.....48

II. MATERIALS AND METHODS51

II-1. Strains and plasmids	51
II-2. Electrotaxis assay.....	51
II-3. Chemotaxis assay.....	52
II-4. Quantitative analysis of cell migration	52
II-5. RT-PCR analysis	53
II-6. Cell Morphology and development	53
III. RESULTS	54
III-1. Identification of the gene encoding SLPC.....	54
III-2. <i>Slpc</i> gene editing with CRISPR/Cas9	56
III-3. Morphology and development of <i>slpc</i> null cell	59
III-4. Electrotaxis of <i>slpc</i> null cell	61
III-5. Chemotaxis of <i>slpc</i> null cell	64
IV. DISCUSSION	66
CONCLUSION.....	67
REFERENCE.....	70

LIST OF FIGURES

GENERAL INTRODUCTION

Figure 1. Diagram depicting hypothetical mechanisms of electrotaxis against chemotaxis
 12

PART I. Phosphatidylinositol 3-kinases play a suppressive role in cell motility of vegetative *Dictyostelium* cells

Figure 1. Motility of wild-type Ax3 cells and *pi3k1/2* null cells in LY294002..... 19

Figure 2. Electrotactic responses of wild-type cells in the presence of LY294002..... 20

Figure 3. Electrotactic responses of *pi3k1/2* null cells in the presence of LY294002..... 23

Figure 4. Electrotactic responses of *pi3k1-5* null cells 24

Figure 5. Random motility of wild-type cells on the vegetative or the aggregation-
 competent conditions..... 27

Figure 6. Random motility of *pi3k1/2* null cells on the vegetative or the aggregation-
 competent conditions..... 28

PART II. Dynamic subcellular localization of DydA in *Dictyostelium* cells

Figure 1. Domain structure and localization of full-length DydA..... 37

Figure 2. Localization of truncated DydA proteins..... 40

Figure 3. Actin foci localization of DydA..... 42

Figure 4. Colocalization of the PRM region and coronin Dual-view analyses of cells
 expressing both GFP-PRM and RFP-coronin..... 44

PART III. Role of Shaker-like potassium channels in cell migration in

Dictyostelium

Figure 1. Shaker-like potassium Channel domain structure and phylogenetic analysis ..55

Figure 2. Targeting of *slpc* gene using CRISPR57

Figure 3. Confirmation of *slpc* knockout cells58

Figure 4. Morphology and Development of the *slpc* null cells60

Figure 5. Electrotactic responses of wild-type cells and *slpc* null cells.....62

Figure 6. Electrotaxis of wild-type cells and *slpc* null cells on the vegetative
 conditions..... 63

Figure 7. Chemotaxis of wild-type cells and *slpc* null cells on the aggregation-competent
 conditions.....65

ABBREVIATIONS

CH	Calponin homology
DB	Develop buffer
DydA	Daydreamer
EF	Electric field
EVH1	Enabled/VASP (vasodilator-stimulated protein) homology
GSK-3	Glycogen synthase kinase-3
MRL	Mig10/RIAM/Lamellipodin
PH	Pleckstrin homology
PI3K	Phosphatidylinositol 3-kinase
PIP2	Phosphatidylinositol 4,5-bisphosphate
PIP3	Phosphatidylinositol 3,4,5-triphosphate
PKB	Protein kinase B
PKBR1	Protein kinase B-related kinase
PPII	Polyproline type II
PRM	Proline-rich motif
RA	Ras associating
SD	Standard deviation
SEM	Standard error of the mean
TORC2	Target of rapamycin complex 2

ABSTRACT

Characterization of PI3Ks, DydA and Shaker-like Potassium Channel Proteins in *Dictyostelium*

Wonbum Kim

Advisor: Prof. Taeck Joong Jeon, Ph.D.

Department of Integrative Biological Science

Graduate School of Chosun University

Directed cell migration is required for diverse cellular processes including immune responses, development, wound healing, and tumor metastasis. While chemotaxis, is relatively well known, electrotaxis, has recently begun to be actively studied. Chemotaxis and electrotaxis share a common signaling pathway for cytoskeleton rearrangements, F-actin-mediated protrusion at the front and myosin-mediated cell contraction at the lateral and the back of migrating cells. However, it is known that the initial stage of detecting external signals operates separately in each of the chemotaxis and electrotaxis. To gain an insight into the mechanism by which cells detect external stimuli in the directional cell migration, this study focuses on understanding the roles of three key signaling molecules in cell migration, PI3K, DydA, and Shaker-like potassium channel protein.

Phosphatidylinositol 3-Kinase (PI3K) is a crucial regulator of cell motility during chemotaxis. It plays a significant role in polarizing cells and amplifying chemoattractant signals to ultimately regulate the rearrangement of the actin cytoskeleton. To investigate whether PI3K has a comparable function in electrotaxis as it does in chemotaxis, I analyzed the directional migration of cells when exposed to an electric field (EF). My findings indicate that the influence

of PI3K on cell motility is contingent on the state of the *Dictyostelium* cells. In the presence of the PI3K inhibitor LY294002, wild-type cells in the vegetative state exhibited increased motility, while cells with the ability to aggregate showed a slight decrease in motility. This result suggests that the effect of LY294002 on cell motility is dependent on the cell's state. Consistent with these results, *pi3k1/2* null cells in the vegetative state showed the same results compared to wild-type cells. These results indicate that PI3K has an inhibitory effect on cell motility in vegetative state *Dictyostelium* cells. This inhibitory effect is reversed when PI3K is inhibited or deficient, resulting in increased motility.

DydA is an adaptor protein that links Ras signaling to cytoskeletal rearrangements and plays an important role in chemotaxis, development, and cell growth. DydA is a downstream effector of RasG and is involved in the regulation of cell polarity during chemotaxis. To understand the mechanism by which DydA functions on the cell migration, I investigated the dynamic subcellular localization of DydA in response to chemoattractant and found that DydA rapidly and transiently translocated to the cell cortex through the RA domain and the PRM region in DydA in response to chemoattractant. The PRM region appears to play a primary role in the translocation of DydA to the cell cortex and in its localization to the actin foci at the bottom of cells. Colocalization experiments of GFP-PRM with RFP-coronin indicated that GFP-PRM preceded GFP-coronin by 2–3 s in response to chemoattractant stimulation. These results suggest that the PRM region plays an indispensable role in relaying upstream regulators, such as RasG, to downstream effectors by mediating the localization of DydA to the cell cortex upon chemoattractant stimulation.

Shaker family proteins, which were initially identified as voltage-gated potassium channel proteins, are involved in neurotransmitter release, heart rate, and muscle contraction. *Dictyostelium* has a Shaker-like potassium channel (SLPC, DDB_G0277011). The BTB domain of SLPC shows 46% amino acid identity with that of Kv1, a potassium voltage-gated shaker channel in mammals. To investigate the functions of SLPC in cell migration, I generated SLPC knock-out cells using CRISPR/Cas9 and all-in-one pTM1285 vectors. I obtained 12 clones,

which were grouped into 5 gene-edited cell strains. One of them had an insertion of 215 bp (*slpc* null cells), which were confirmed by sequencing and PCR reactions using genomic DNAs and gene-specific primers. The cell line was employed in the subsequent experiments to explore the phenotypes associated with development and cell migration. *slpc* null cells were smaller than wild-type cells. In electrotaxis using vegetative state cells, *slpc* null cells showed directional migration to the cathode as wild-type cells do with a similar directionality in response to electric fields (EF). However, *slpc* null cells migrated with a slightly decreased speed compared to wild-type cells. When the aggregation-competent cells were used in electrotaxis, cells lacking SLPC showed similar phenotypes, normal directionality and decreased speed, to those in vegetative state cells. In chemotaxis, *slpc* null cells exhibited no significant difference compared to wild-type cells. In development, *slpc* null cells displayed aberrant multicellular structures after normal aggregation stage of development. These results suggest that SLPC plays some roles in electrotaxis and development. In this study, I characterized three key signaling molecules, PI3Ks, DydA, and SLPC, in directed cell migration. The results of this study will contribute to understand the initial signal transduction stage of detecting the external signals in both chemotaxis and electrotaxis.

초록

세포이동에서 PI3Ks, DydA 및 Shaker-like 칼륨 채널 단백질의 역할 규명

김 원 범

지도교수 : 전 택 중

글로벌바이오융합학과

조선대학교 대학원

방향성 세포 이동은 면역반응, 발달, 상처치유, 종양전이 등 다양한 생리학적 과정에서 필요하다. 주화성이동은 잘 알려져 있지만 주전성이동은 최근 활발하게 연구되기 시작했다. 주화성이동과 주전성이동은 세포 골격 재배열, 이동하는 세포의 앞쪽의 F-액틴 돌출과 측면, 뒤쪽의 마이오신에 의해 유도되는 수축을 위한 공통된 신호 경로를 가지고 있다. 그러나 외부 신호를 감지하는 초기 단계는 주화성이동과 주전성이동에서 각각 개별적으로 작동하는 것으로 알려져 있다. 본 연구는 세포가 외부자극을 감지하여 세포의 이동 방향을 유도하는 기전을 조사하기 위해 세포 이동에 있어 핵심분자인 PI3K, DydA, Shaker 유사 칼륨 채널 단백질의 역할을 이해하고자 한다.

PI3K 는 주화성이동을 할 때에 세포의 운동성을 조절하는 인자이다. 이 효소는 세포를 극성화하고 화학적 신호를 증폭하여 액틴 골격의 재배열을 조절하는 역할을 한다. PI3K 가 주화성이동과 마찬가지로 주전성이동에서 비슷한 기능을 하는지

알아보기 위해 전기장(EF)의 자극에서 세포의 이동을 분석하였다. 나의 연구 결과는 *Dictyostelium* 세포의 상태에 따라 PI3K가 세포 운동성에 미치는 영향이 달라진다는 것을 나타낸다. PI3K 억제제인 LY294002가 존재할 때 식물 상태의 야생형 세포는 운동성이 증가한 반면, 응집 능력이 있는 세포는 운동성이 약간 감소했다. 이 결과는 LY294002가 세포 운동성에 미치는 영향이 세포의 상태에 따라 달라진다는 것을 시사한다. 이러한 결과와 일관되게, 식물성 상태의 *pi3k1/2* 결핍세포는 야생형 세포와 동일한 결과를 보였다. 이러한 결과는 PI3K가 식물성 상태의 *Dictyostelium* 세포에서 세포 운동성을 억제하는 효과가 있음을 나타낸다. 이러한 억제 효과는 PI3K가 억제되거나 결핍되면 역전되어 운동성이 증가한다.

DydA는 Ras 신호와 세포 골격 재배열을 연결하는 어댑터 단백질로 화학 주성, 세포 발생 및 성장에 중요한 역할을 한다. DydA는 RasG의 하류 반응기이며 주화성이동 동안 세포 극성 조절에 관여한다. DydA가 세포 이동에 작용하는 기전을 이해하기 위해 화학 유인제에 반응하는 DydA의 시공간적 재배열을 조사하였다. 주화성 자극에 반응하여 DydA가 RA 도메인과 PRM 영역을 통해 세포 피질로 빠르고 일시적으로 이동하는 것을 발견했습니다. PRM 영역은 DydA가 세포 피질로 이동되고 세포 바닥의 액틴 집단으로 이동하는데 주요 역할을 하는 것으로 보인다. GFP-PRM과 RFP-coronin의 시공간적 재배열을 조사한 결과 주화성 자극에 반응해 GFP-PRM이 RFP-coronin보다 2~3초 빠르게 재배열 되는 것으로 나타났다. 이러한 결과는 PRM 영역이 주화성 자극에 따라 세포 피질로 DydA의 이동을 매개하여 RasG와 같은 상위 인자를 하류 반응기로 전달하는데 필수적인 역할을 한다는 것을 시사한다.

Shaker는 전압 차폐 칼륨 채널로 신경전달물질 방출, 심박수 및 근육 수축에 관여한다. *Dictyostelium*은 Shaker와 유사한 칼륨 채널(SLPC, DDB_G0277011)을 가지고 있다. SLPC의 BTB 도메인은 포유류의 칼륨 전압 게이트 Shaker 채널인 Kv1과 46%의 아미노산

동일성을 보였다. 세포 이동에서 SLPC의 기능을 조사하기 위해 CRISPR/Cas9 및 올인원 pTM1285 벡터를 사용하여 SLPC 녹아웃 세포를 생성하였다. CRISPR/Cas9 유전자 편집 실험에서 12개의 클론을 얻었으며, 이를 5가지의 유전자 편집 세포 균주로 분류하였다. 그 중 하나를 게놈 DNA와 유전자 특이 프라이머를 사용한 시퀀싱 및 PCR 반응으로 확인된 215bp (*slpc* null 세포)의 삽입을 확인하였다. 이 세포주는 다음 실험에서 발달과 세포 이동의 표현형을 조사하는 데 사용되었다. *slpc* null 세포는 야생형 세포보다 훨씬 작았다. 식물 상태 세포를 이용한 주전성 세포 이동에서 *slpc* null 세포는 야생형 세포와 마찬가지로 EF에 반응하여 비슷한 방향성을 가지고 음극으로 이동하는 것으로 나타났다. 그러나 *slpc* null 세포의 이동 속도는 야생형 세포에 비해 약간 낮았다. 응집 능력 상태에서는 주전성 운동은 방향성이 있었지만 운동성이 떨어졌고, 주화성 이동도 비슷한 결과를 보였습니다. 발달 과정에서 *slpc* null 세포는 정상적인 응집 단계 이후 비정상적인 다세포 구조를 나타냈다. 이러한 결과는 SLPC가 주전성 이동 및 발달에 어떤 역할을 한다는 것을 시사한다. 본 연구 결과는 PI3Ks, DydA, SLPC의 특성을 파악함으로써, 주전성 이동과 주화성 이동 사이에 특이적인 네트워크 신호 전달의 생물학적 과정을 이해하는데 기여할 것으로 기대된다.

GENERAL INTRODUCTION

1. Cell migration

Cell migration is a crucial phenomenon underlying various biological and pathological processes, ranging from embryonic development to wound healing, inflammatory responses, and tumor metastasis (Jin et al., 2009; Lee and Jeon, 2012b; Ridley et al., 2003). It is speculated that the origin of cell migration is an escape from nutrient depletion and that it was evolved and adopted to a variety of current biological processes. In the microbial realm, bacteria and many free-living eukaryotic cells, such as protozoa, move with flagella, cilia, or related appendages. Conversely, amoebae and most metazoan cells utilize morphological extensions like pseudopodia, lamellipodia, or blebs for locomotion, and some of cells have cilia and cells such as sperm rely on flagella for propulsion.

A multiplicity of external stimuli drives the directed migration of cells, including light (Armitage and Hellingwerf, 2003), chemicals (Bagorda and Parent, 2008), mechanical forces (Lo et al., 2000), electric fields (Gao et al., 2011; Zhao et al., 2006), and temperature (Ramot et al., 2008; Whitaker and Poff, 1980). The reconstitution of the actin cytoskeleton is essential for cell migration. In addition, this molecular mechanism controlling migration of cells is evolutionarily conserved across different organisms, from eukaryotic cells to human leukocytes. However, it is difficult to understand cell migration because it requires the integration and temporal coordination of diverse processes occurring in spatially different locations within the cell (Lee and Jeon, 2012b). Thus, there is considerable interest in elucidating the fundamental mechanisms governing cell migration.

The cell movement is mediated by a coordinated regulation of the cytoskeleton, F-actin-mediated protrusions at the front of the cell and myosin II-mediated contraction of the cell posterior (Ridley et al., 2003).

1-1 Assembly of the actin cytoskeleton

The actin cytoskeleton, organized around the cell cortex, is the driving force for cellular movement and serves as the ultimate destination for chemotactic signaling. The leading edge of the cell migration localizes the higher proportion of F-actin, while a comparatively lower proportion localizes at the posterior. Crucial regulators of lamellipodia and filopodia formation at the leading edge are the Rho family small GTPases, including Rho, Rac, and Cdc42 proteins, found ubiquitously in mammalian cells. Upon activation, these GTPases interact with downstream targets such as protein kinases, lipid-modifying enzymes, and activators of the Arp2/3 complex, intricately orchestrating cell motility.

Rac and Cdc42 play a central role with the WASP/WAVE family proteins, which are Arp2/3 complex activators, as their primary targets for actin polymerization at protrusion. WASP/WAVE proteins bind to activated Rac proteins and stimulate the Arp2/3 complex to mediate dendritic actin polymerization. The dynamic interplay of these interaction component highlights the complexity of cellular movement (Firat-Karalar and Welch, 2011; Ridley et al., 2003; Rodal et al., 2005; Stephens et al., 2008).

However, this complicated system is affected by modulation and complexity, as shown by the recently discovered inhibitor of the Arp2/3 complex, Arpin, which acts in opposition to SCAR. Additionally, in the absence of SCAR, cells can exhibit movement mainly through blebs, replacing SCAR with WASP in the remaining pseudopods. The signaling route from chemoattractant receptors to actin polymerization remains an area of active investigation, with the role of specific RhoGEFs and mutants of the Dock/Zizimin family of GEFs providing insights into defects in movement or actin polymerization.

1-2 Assembly of myosin II cytoskeleton

Assembled myosin II is predominantly located at the rear of the cell and along the lateral sides during cell movement, with a decreasing gradient from posterior to anterior. Assembled

myosin II is concentrated at the rear and lateral regions of mobile cells. Assembled myosin II plays a crucial role in maintaining cortical tension along the cell's sides, thereby preventing the formation of lateral dendrites (Ridley et al., 2003; Stephens et al., 2008). Myosin II is a significant negative regulator of leading-edge function, which confines the initiation site of dendrite formation specifically to the leading edge of motile cells (Lee et al., 2010; Meili et al., 2010). For the cell to sustain continuous motility, it must disengage adhesive contacts at the posterior floor and contract the rear portion, a process dependent on the motor activity of myosin II. In *Dictyostelium* cells lacking myosin II, the retractions of the cell's posterior during chemotaxis are impaired, resulting in an abnormal loss of lateral cortical tension. This deficiency leads to the development of lateral pseudopodia and inefficient chemotaxis (Bosgraaf and van Haastert, 2006; De Lozanne and Spudich, 1987). Myosin II is additionally concentrated at the cell's posterior and plays a role in posterior contraction in fibroblasts and neutrophils (Xu et al., 2003). *Dictyostelium* myosin II, the extensively investigated conventional non-muscle myosin, exhibits a molecular structure remarkably akin to that of mammalian myosin II. The C-terminal coiled-coil regions of two myosin II monomers intertwine to form a bipolar dimer. The assembly of these dimers into myosin filaments is, in part, regulated by the phosphorylation of three threonine residues in the tail region, a process mediated by myosin heavy chain kinases (MHCKs). Phosphorylation leads to filament disassembly, while dephosphorylation promotes assembly (Bosgraaf and van Haastert, 2006; Kortholt and van Haastert, 2008). Furthermore, the regulation of myosin II assembly at the posterior of mobile cells involves mediation through PAKa and the cGMP pathway (Kortholt and van Haastert, 2008).

2. *Dictyostelium* as a model organism for cell migration

Dictyostelium discoideum is a suitable model organism for studying cellular processes, including cell migration, cell division, and multicellular development. It is a powerful model system for investigating chemotaxis, the directional movement of cells towards chemoattractants. *Dictyostelium* is a free-living soil amoeba that feeds on bacteria. These organisms follow bacteria

by chemotaxing towards folic acid, which is secreted by the bacteria (Chisholm and Firtel, 2004b). This process is very similar to macrophages or neutrophils chasing bacteria. In the state of starvation, *Dictyostelium* experiences a strictly regulated multicellular developmental process in which they secrete cAMP and move toward aggregation centers through chemotaxis, finally forming fruiting bodies (Chisholm and Firtel, 2004b).

3. Principle of chemotaxis in *Dictyostelium*

The initiation of chemotaxis in *Dictyostelium* is the binding of a chemoattractant to a G-protein coupled receptor (GPCR) located on the cell surface. Upon ligand binding, the GPCR sets off a cascade of signaling pathways, engaging various molecules to coordinate cell migration toward the source of chemoattractant (Kolsch et al., 2008; Kortholt and van Haastert, 2008).

The fundamental cycle of cell migration involves the extension of a protrusion in the direction of movement, the establishment of a stable attachment near the leading edge of the protrusion, and the subsequent release and retraction of the attachment at the rear of the cell. This cyclic process leads to the forward movement of the cell body. The orchestration of cell migration depends on the coordinated regulation of the cytoskeleton, with F-actin-mediated protrusions at the cell's front and myosin II-mediated contractions at its rear playing pivotal roles (Ridley et al., 2003).

Ras activation constitutes an early response to chemoattractant stimulation downstream of receptors and heterotrimeric G proteins. The activated Ras protein concentrates at the leading edge of stimulated cells, initiating localized activation of signaling molecules, including phospho-phosphatidylinositol 3-kinase (PI3K). The co-localization and activation of PI3K and PTEN cause the accumulation of phosphatidylinositol (3,4,5) trisphosphate (PIP3). This accumulation facilitates the recruitment of pleckstrin homology (PH) domain-containing proteins such as PhdA, CRAC, and PKB, leading to the localized polymerization of F-actin and

the extension of pseudopods (Kortholt and van Haastert, 2008; Raaijmakers and Bos, 2009; Sasaki et al., 2004).

4. Principle of electrotaxis in *Dictyostelium*

Cells exhibit directional migration in response to different extracellular cues such as chemical gradients (chemotaxis), topography, mechanical forces (mechanotaxis/durataxis), and electrical fields (EFs) (electrotaxis/galvanotaxis). This paper delves into the significant impact of electrotaxis, the directional migration of cells in response to electric fields, on cellular behavior across diverse physiological settings (Mycielska and Djamgoz, 2004; Pongs and Schwarz, 2010). Electrotaxis is increasingly recognized for its relevance in essential processes like embryonic development, nerve cell growth induction, wound healing, angiogenesis, and the guidance of metastatic cancer cells. Electric fields that are controlled in microseconds can modulate cell position by accurately and rapidly adjusting the directional movement of the cells in response to a stimulus. These advantages allow electric fields to be used as versatile guidance tools, such as chemoattractants.

Despite initial insufficient studies of electrotaxis *in vivo*, continuing evidence suggests that it is related in important cell movement essential for functional processes such as development, morphogenesis, and regeneration. For instance, disruption of epithelial integrity induces the spontaneous generation of an electric field oriented towards the wound, triggering directional migration of surrounding epithelial cells to cover the wounded tissue. Although the mechanisms of how cells sense weak direct current electric fields are not fully understood, but there is growing interest to study this mechanism.

The paper acknowledges the complexity of electrotaxis, influenced by factors like cell type, medium conditions, and diverse intracellular signaling cascades. While the molecules determining migration direction in electrotaxis remain unidentified, the paper emphasizes the potential therapeutic applications of electrotaxis in wound healing and tissue repair. Extensive

research is needed to elucidate the physiological mechanisms of electrotaxis in a variety of cell types and organisms and to contribute to a more comprehensive understanding of the full therapeutic potential of electrotaxis in diverse biological contexts.

5. The role of PI3Ks in *Dictyostelium*

PI3Ks (Phosphatidylinositol 3-Kinase) signaling plays a dynamic and pivotal role at the leading edge of the cell, where it coordinates cellular movements by regulating cytoskeleton polymerization. These intracellular signal transducer enzymes, belonging to the PI3K family, possess the ability to phosphorylate the 3-position hydroxyl group of the inositol ring of phosphatidylinositol (PI). In the of *Dictyostelium*, a model system for cellular processes, PI3Ks are comprised of six subunits: pikA, pikB, pikC, pikF, pikG, and pikH (Gao et al., 2015a).

The PI3K pathway, including the oncogene PIK3CA and the tumor suppressor gene PTEN, is involved in diverse cellular processes and is particularly relevant in determining the sensitivity of cancer tumors to insulin and insulin-like growth factor 1 (IGF1). The pathway's influence extends to the regulation of phosphatidylinositol 4,5-bisphosphate (PIP2) phosphorylation to phosphatidylinositol 3,4,5-trisphosphate (PIP3), affecting proteins containing a pleckstrin homology (PH) domain. The phosphorylated PIP3 is a key regulator in controlling cell motility (Hoeller and Kay, 2007; Sasaki and Firtel, 2006).

Targets of PIP3 include substrates of Akt, such as PAK (p21-activated kinase), and various PH domain-containing proteins. Phosphorylated PIP3 is actively involved in the regulation of cell motility, as evidenced by the appearance of spontaneous PIP3 patches on protrusions, especially in cells undergoing random movement. This underlines the dynamic and localized characteristic of PI3K signaling (Hoeller and Kay, 2007). In *Dictyostelium*, PI3K is recruited to these regions, while PTEN is lost from them. Additionally, the 5'-phosphatase Ship1 in neutrophils also contributes to PIP3 degradation. The accumulation of PIP3 activates molecules interacting with it, influencing cellular trafficking through multiple cells signaling pathways. The

intricate regulation of PI3K signaling, as observed in various cellular processes, highlights its significance in regulating fundamental cellular movements.

6. Daydreamer of *Dictyostelium*

Daydreamer (DydA), an adaptor protein belonging to the Mig10/RIAM/lamallipodic family, serves as an important Ras effector, playing a pivotal role in cell polarization and orientation during gastrulation. glycogen synthase kinase-3 (GSK-3) is responsible for phosphorylating DydA, a modification essential for some but not all, of its functions (Kolsch et al., 2013).

In the *Dictyostelium*, GSK-3 was first identified through a genetic screen focused on regulators of cell fate determination. Subsequent studies established its significance in chemotaxis, highlighting its multifaceted role. Cells deficient in GSK-3 (*gskA*⁻) exhibit notable alterations in behavior compared to their wild-type cell. Specifically, *gskA*⁻ cells show reduced speed and significantly decreased directionality, underlining the importance of GSK-3 in cellular dynamics (Baumgardner et al., 2018; Kim et al., 2017; Kolsch et al., 2013).

Furthermore, the absence of GSK-3 in these cells results in a diminished production of the PI3K product phosphatidylinositol (3,4,5)-triphosphate (PIP3). This reduction is entrained by decreased phosphorylation of the activation loop (AL) of Akt/PKB and the related kinase PKBR1. These findings illuminate the interconnected regulatory network in which GSK-3 operates, influencing both cell motility and intracellular signaling pathways (Baumgardner et al., 2018).

7. Shaker

The shaker (Sh) protein, found in *Drosophila melanogaster*, causes a variety of abnormal behaviors when mutated. The mutant flies, under ether anesthesia, show shaking their legs, a trait from which the gene derives its name. Even in an unanesthetized state, these mutant flies exhibit irregular movements and have a reduced lifespan compared to their regular counterparts (Wang et al., 1994).

The larvae of Sh-mutant flies manifest repetitive firing of action potentials and prolonged exposure to neurotransmitters at neuromuscular junctions. Notably, the shaker gene, located on the X chromosome in *Drosophila*, shares its closest human homolog, KCNA3 (McLaughlin and Levin, 2018b).

Exploring the shaker gene in fruit flies provides valuable insights into the genetic foundations of behavior and neurophysiological processes, potentially offering relevance to human genes and health. Voltage-gated potassium (Kv) channels, a diverse group of ion-selective channels in excitable cell membranes, play crucial roles in mature neurons, determining resting membrane potentials, shaping action potentials, regulating firing patterns, and neurotransmitter release (Manganas and Trimmer, 2000).

While the roles of Kv channels are well-studied in mature organisms, the roles during embryogenesis are poorly defined. Developmentally regulated potassium (K^+) currents, observed in nonmammalian species at various embryonic stages, include the delayed rectifier K^+ current (IKv). This current, detected during neurogenesis in amphibians, is crucial for the transition from early, long-duration action potentials to mature, brief spikes.

Expression of *Xenopus* Kv1.1 (xKv1.1) plays an important role in the development of IKv and has an impact on neuronal development. xKv1.1 and xKv2.2, homologous to mammalian Kv channels, expressed in developed *Xenopus* spinal neurons. Overexpression of xKv1.1 in cultured spinal neurons results in the premature appearance of IKv and a reduction in morphologically differentiated neurons. Temporal regulation of xKv1.1 and xKv2.2 transcripts in developing spinal neurons further emphasizes their role in IKv development (Bosgraaf et al., 2008; Wang et al., 1994).

These findings collectively suggest the potential significance of xKv1.1 in the complicated processes of potassium current development and, by extension, neuronal maturation. Understanding these mechanisms contributes to broader insights into neural development and the establishment of functional neural circuits.

8. Chemotaxis and electrotaxis have a shared signaling pathway

In the realms of cellular movement, chemotaxis and electrotaxis stand as distinct yet interconnected phenomena, steering cells in specific directions in response to diverse external stimuli. Despite the uniqueness of their triggers, both processes share a central signaling network characterized by the involvement of TORC2 (Target of Rapamycin Complex 2) and PI3K (Phosphoinositide 3-Kinase). This shared network serves as a connection for modulating the intricate signaling of cellular movement in response to both chemical and electrical stimulation. (Fig. 1.)

However, there are some differences between chemotaxis and electrotaxis in their shared signaling pathways. Both processes involve TORC2 and PI3K, as well as certain receptors such as the cAMP receptor cAR1. However, the G β subunit of trimeric G-proteins, which is downstream of the cAMP signaling pathway, is essential for chemotaxis but not for electrotaxis. These distinct characteristics suggest that there are shared pathways and stimulus-specific pathways. Understanding the commonalities and differences in the mechanisms for chemotaxis and electrotaxis provides a deeper understanding of the fundamental signaling pathways in these cellular processes. In electrotaxis, electric fields activate the major shared signaling network and a specific pathway unidentified yet. converge on the cytoskeletal network, a crucial component altered during both chemotaxis and electrotaxis. Changes in the cytoskeleton network lead to cell movement and directed migration. Recently conducted studies imply that G β subunit of G proteins regulates the speed of movement, and RasG regulates directionality during electrotaxis. Recently, a screening study in *Dictyostelium* identified a range of genes crucial for electroaxis movement (Runchi Gao et al., 2015). These include PiaA, GefA, RasC, Rip3, Lst8, and PKBR1 (Gao et al., 2015a). PiaA is a crucial part of TORC2, a protein complex of kinases that transmits changes in motility by activating Akt/PKB. Mutants that lack gefA, rasC, rip3, lst8, and pkbR1 genes encoding other components of the TORC2-PKB pathway display reduced electrogenicity.

Beyond its involvement in electrotaxis, PiaA has a critical role in the stimulation of adenylyl cyclase (ACA) and the activation of PKB. These findings indicate that there exist shared signalling pathways, which regulate both chemotaxis and electrotaxis, consequently affecting the formation of the cytoskeleton.

During directional cell movement, an intermittent and gradual rise in intracellular Ca^{2+} levels in moving cells often occurs, with a correlation to the direction of movement. Chemotaxis facilitate the rapid influx of Ca^{2+} across the cell membrane, resulting in elevated intracellular Ca^{2+} in a variety of cell types, including *Dictyostelium discoideum*. The role of Ca^{2+} signaling is widely recognized to be a key regulator of cell migration in response to chemical gradients. The disruption of the inositol 1,3,5-trisphosphate [Ins(1,3,5)P₃]-receptor-like gene *iplA* in *Dictyostelium* cells results in the abolition of intracellular free calcium concentration ($[\text{Ca}^{2+}]_i$) elevation in response to chemoattractants such as cAMP or folate. Interestingly, despite this disruption, the chemical migration of *iplA*-deficient cells towards cAMP and folate sources remains unaffected. In Electrotaxis, the absence of directional migration was observed when there was no increase in intracellular free calcium concentration ($[\text{Ca}^{2+}]_i$). Notably, while the elevation of $[\text{Ca}^{2+}]_i$ by chemoattractants is not a prerequisite for chemical migration, electrotaxis relies on EF-induced elevation of $[\text{Ca}^{2+}]_i$ due to calcium influx.

A membrane hyperpolarized by a voltage-gated channel and facing the anode attracts Ca^{2+} via electrochemical diffusion. As a result, contraction occurs at the back of the cell, pushing the cell toward the cathode. Conversely, in cells with voltage-gated Ca^{2+} channels, these channels open near the cathode (depolarizing) side, facilitating Ca^{2+} influx. The interaction between calcium dynamics and membrane potential forms the basis of electrotaxis. The direction of cell movement depends on the balance between the opposing contractile forces generated on each side. While it has been proposed that changes in membrane potential (V_m) may underlie electrotaxis, the direct testing of the role of V_m in electrotaxis has yet to be conducted.

To study the mechanisms of directional cell migration, it is necessary to investigate the factors that sense direction and polarize cells. These results are essential for comprehending the

mechanisms underlying electrotaxis. By scrutinizing the pathways upstream of the PI3K pathway, a signaling pathway shared by both cell migration models, I can reveal differences, if any, in the signaling pathway. This paper aims to identify the initial signaling pathways of electrotaxis and chemotaxis by characterising PI3K, DydA (RasG-associated adaptor protein), and shaker-like potassium channels that have significant roles in chemotaxis.

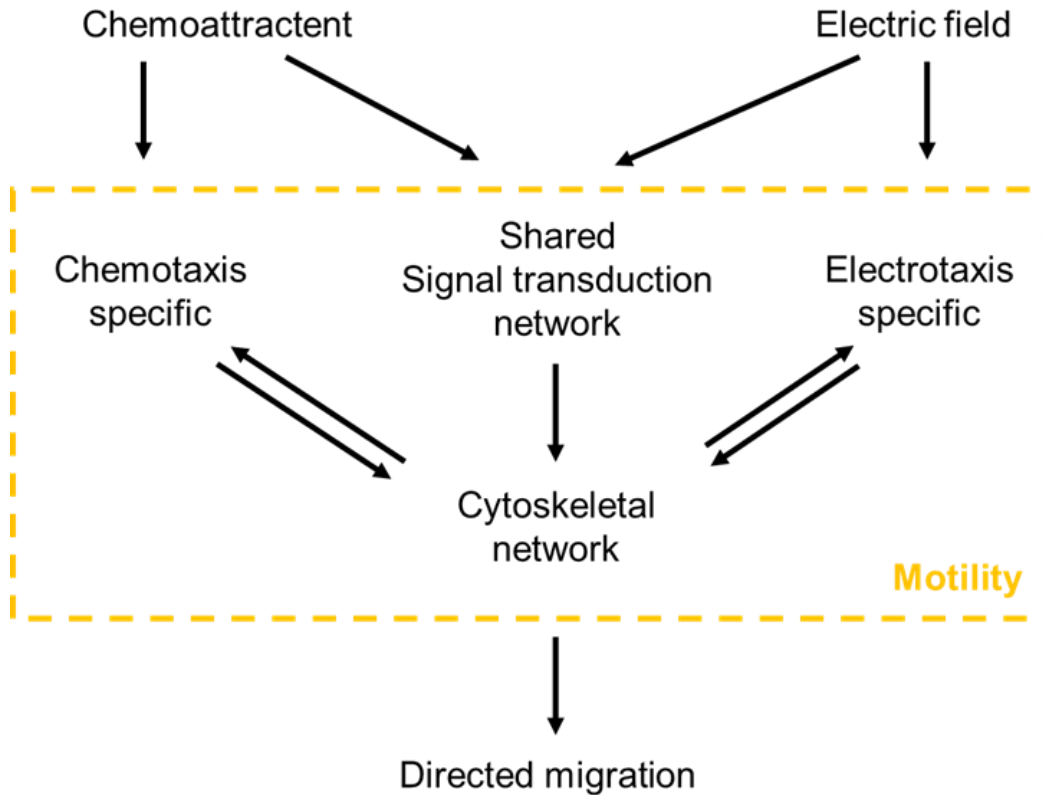


Fig. 1. Diagram depicting hypothetical mechanisms of electrotaxis against chemotaxis

The diagram outlines the comparative mechanisms of electrotaxis and chemotaxis, emphasizing shared signaling pathways like TORC2 and PI3K, specific components such as cAR1 and G β in chemotaxis, unidentified electric field receptors in electrotaxis, and the converging role of cytoskeletal networks, providing insights into their nuanced cellular responses.

This part has been published as Wonbum Kim and Taeck J. Jeon, 2022

PART I. Phosphatidylinositol 3-kinases play a suppressive role in cell motility of vegetative *Dictyostelium* cells

I. INTRODUCTION

Directed cell migration is induced by various external stimuli. Electrotaxis is directional cell migration in an electric field (EF) and is involved in a wide range of physiological processes, such as embryogenesis, neuronal guidance, wound healing, and metastasis (McLaughlin and Levin, 2018a; Tai et al., 2018; Zhao, 2009b). The molecular mechanism of directional cell migration has been revealed to be based primarily on chemoattractant-directed cell migration. G-protein coupled receptors at the cell surface relay external chemoattractant signals as intracellular secondary signals that mediate cytoskeleton rearrangement through multiple signaling pathways, including phosphatidylinositol 3-kinase (PI3K), TORC2 complex, phospholipase A2, and phospholipase C. The differential activation of these signaling transduction cascades leads to the local polymerization of F-actin and membrane protrusion at the leading edge of cells, mediating directional cell migration up a gradient of chemoattractants (Artemenko et al., 2014; Kolsch et al., 2008). The detailed molecular mechanisms underlying EF-directed cell migration remains unclear. However, the major signaling networks, including the PI3K/PIP3 and TORC2/PKB pathways, involved in cytoskeleton rearrangements during chemotaxis are generally thought to be commonly used in the process of electrotaxis (Gao et al., 2015b; Tai et al., 2018; Zhao, 2009b).

PI3K is a key signaling molecule in cell migration and other cellular pathways, including growth, survival, proliferation, and vesicle trafficking (Artemenko et al., 2014; Khezri et al., 2022; Koch et al., 2021). PI3Ks preferentially localize to the leading edge of migrating cells in response to chemoattractant stimuli and phosphorylate the 3 position of phosphatidylinositol 4,5-bisphosphate (PIP₂) to produce phosphatidylinositol 3,4,5-triphosphate (PIP₃) at the plasma

membrane. PIP₃ asymmetrically accumulated at the leading edge of migrating cells contributes to preferential F-actin assembly and membrane protrusion by recruiting signaling molecules involved in the regulation of the actin cytoskeleton in the cytosol (Artemenko et al., 2014; Funamoto et al., 2002; Funamoto et al., 2001; Kolsch et al., 2008). PI3K pathway is also involved in EF-directed cell migration. PI3K in keratinocytes, as in chemoattractant stimulation, are activated by the application of EF, producing PIP₃ and activating AKT. EF-induced directional migration of epithelium cells during wound healing is abolished by genetic disruption of PI3K (p110), the catalytic subunit of PI3K γ (Zhao et al., 2006).

Dictyostelium discoideum, a model organism for the study of cell migration, shows strong directional movements in response to external electric fields and chemoattractants such as folate and cAMP (Artemenko et al., 2014; Zhao et al., 2002). Recently, many genes such as PiaA, GefA, RasC, Rip3, Lst8, and PKBR1 that are required for electrotaxis have been identified in a large-scale screening study of *Dictyostelium* (Gao et al., 2015b). Analyses of the acceleration/deceleration kinetics of directionality and migration speed in EF-directed cell migration showed that migration speed and directionality were separately regulated by G β and RasG, respectively (Jeon et al., 2019). Guanylyl cyclases, GbpC, and PI3K are also involved in the regulation of the directionality of migrating cells in electrotaxis. The direction of cell migration in response to EF was reversed by genetic modulation of guanylyl cyclases and GbpC in combination with the inhibition of PI3Ks (Sato et al., 2009). Accumulating evidence indicates that PI3K plays an important role in directional sensing and polarity formation in response to chemoattractant stimuli, and also suggests that it may play a crucial role in EF-induced cell migration as in chemotaxis. However, the role of PI3K in EF-directed cell migration is yet to be characterized. Here, I investigated the roles of PI3Ks in *Dictyostelium* cell migration. Unexpectedly, my data suggest that PI3Ks play different roles in regulating cell motility, depending on the developmental stage of the cells.

II. MATERIALS AND METHODS

II-1. Strains and cell culture

D. discoideum cells such as wild-type Ax3 cells (DBS0236487), wild-type Ax2 cells (DBS0237914), *pi3k1/2* null cells (DBS0236766), and *pi3k1-5* null cells (DBS0252652) were obtained from the *Dictyostelium* Stock Center (DictyBase). LY294002 and dimethyl sulfoxide (DMSO) were purchased from Sigma-Aldrich (USA). Stock solution of LY294002 (50 mM) was prepared in DMSO and then added to a final concentration of 30 μ M. All the cells were cultured axenically in HL5 medium at 22 °C. The knockout strains were maintained in 10 μ g/ml of blasticidin or G418.

II-2. Electrotaxis and quantitative analysis

Electrotaxis using vegetative cells starved for 3 h was performed as described previously (Gao et al., 2015b; Jeon et al., 2019). Fully grown cells on 24 well plates were washed three times and starved for 3 h in development buffer (DB; 5 mM Na₂HPO₄, 5 mM KH₂PO₄, 2 mM MgCl₂ and 1 mM CaCl₂) and then subjected to electrotaxis experiments. For experiments with aggregation-competent cells, exponentially growing cells were washed twice and resuspended at a density of 5×10^6 cells/mL in DB buffer. The cells were pulsed with 30 nM cAMP every 6 min for 6 h (Jeon et al., 2007). All procedures were carried out at room temperature (~ 22 °C). The prepared cells were seeded in an electrotactic chamber for 20 min and the unattached cells were washed off using DB buffer. A roof of cover glass was placed on the cells within a trough and sealed with silicone grease. Each chamber was then filled with sufficient DB buffer. EF was applied at the indicated field strength through agar salt bridges. For electrotaxis in the presence of LY294002, DB buffer containing 30 μ M LY294002 was prepared and used for all procedures after seeding the cells on the bottom of an electrotactic chamber. Cell migration was recorded at

intervals of 1 min for 1 h using an inverted microscope (IX71; Olympus) with a camera (DS-Fil; Nikon) controlled by the NIS-Elements software (Nikon).

Time-lapse recordings of cell migration were analyzed using ImageJ (National Institutes of Health) as previously described (Gao et al., 2015b; Jeon et al., 2019). Directedness quantifies how directionally cells migrate in response to an EF. The directedness of the movement of the cells was measured as cosine θ , where θ is the angle between the direction of the field and a straight line connecting the start and end positions of the cell. Trajectory speed was assessed by dividing the total distance travelled by the cell by time. All data were obtained and analyzed from at least three independent experiments. The kinetics of directedness and trajectory speed were calculated by measuring the directedness and trajectory speed of cell migration every 2 min in a time-lapse recording and sequentially plotting the readings against time (Jeon et al., 2019).

II-3. Random migration

Vegetative and aggregation-competent cells were prepared as described in the electrotaxis experiments. 1~2 drops of the cell suspension were added to a 30 mm culture plate containing 3 mL of DB buffer without or with 30 μ M LY294002 and allowed to adhere to the plate for 30 min. Images were collected for 30 min and trajectory speed was calculated using ImageJ software (NIH) following the same methods used in the electrotaxis experiments.

II-4. Statistics

Statistical analysis was performed using Student's t-test. All data from at least three independent experiments are expressed as mean \pm SEM, and a P-value less than 0.05 was considered statistically significant.

III. RESULTS

III-1. Electrotaxis of wild-type cells in the presence of LY294002

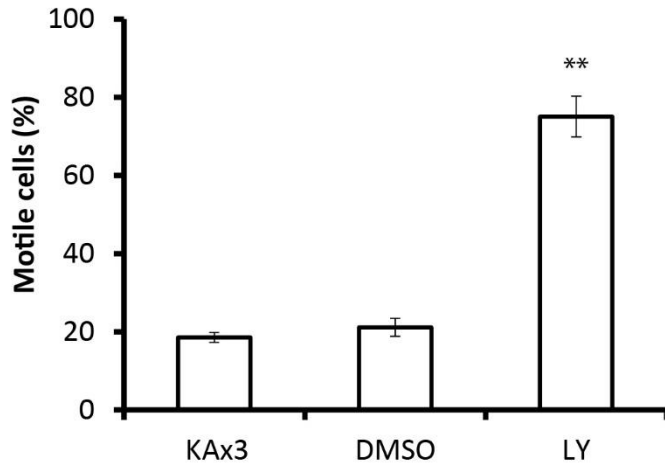
PI3K is involved in directional sensing and signal transduction in chemotaxis (Artemenko et al., 2014; Funamoto et al., 2002). To determine whether PI3K plays a similar role in EF-directed cell migration as in chemotaxis, I examined directional cell migration in response to an EF in the presence of LY294002, a PI3K inhibitor. In the cell migration assay, I used a recently developed method for electrotaxis using 3 h starved cells (Gao et al., 2015b; Jeon et al., 2019). The 3 h starved *Dictyostelium* cells showed directional cell migration in response to external electrical stimuli but not cAMP chemoattractant stimuli.

Cell migration was monitored for 60 min. No EF was applied for the first 10 min, 15 V/cm EF was applied for the following 30 min, and cell migration was recorded without EF stimulation for the final 20 min. Initially, most wild-type cells showed no movement, appearing non-motile and adhered to the plate. Approximately 20 % of wild-type Ax3 cells showed movements during recording and were analyzed for directional migration in response to external EF stimulation (Fig. 1A). Before EF stimulation, the wild-type cells exhibited random migration (approximately 1 $\mu\text{m}/\text{min}$ of trajectory speed and 0 of directedness). Upon EF stimulation, wild-type cells showed directional migration towards the cathode (Fig. 2), and the migration speed and directedness increased to approximately 3.5 $\mu\text{m}/\text{min}$ and 0.6, respectively (Fig. 2A and 2B). Analysis of the influence of EF stimulation over time on cell migration revealed a specific acceleration/deceleration kinetics with regard to directionality and trajectory speed (Fig. 2C). Wild-type cells showed a gradual increase in speed and directionality, reaching the highest recorded values within 5 min of application of EF stimulation; the values returned to the basal level within 5 min of withdrawal of the EF.

Surprisingly, when LY294002, an inhibitor of PI3K, was added to the buffer, most of the cells became motile and displayed increased motility. Approximately 80 % of the cells were motile in the presence of LY294002 compared with the mere 20 % in the absence of LY294002 (Fig. 1).

DMSO treatment did not produce any significant difference in the motility of the cells. Quantification of the motile cells showed that the migration speed of the cells was highly increased in the presence of LY294002 when compared with that of the control cells, which were in the absence of LY294002 or in the presence of DMSO (Fig. 2A). The presence of LY294002 produced an approximate 2-fold increase in speed compared with that of the controls, despite the acceleration/deceleration kinetics of the trajectory speed being similar (Fig. 2C). No significant difference in directionality was detected when cells were treated with LY294002. These data indicate that LY294002 treatment induced motility in cells and increased the migration speed during both random migration and EF-directed migration, suggesting that inhibition of PI3Ks by LY294002 increases cell motility by possibly blocking the inhibitory effect that PI3Ks exert on cell migration in the 3 h starved cells.

A



B

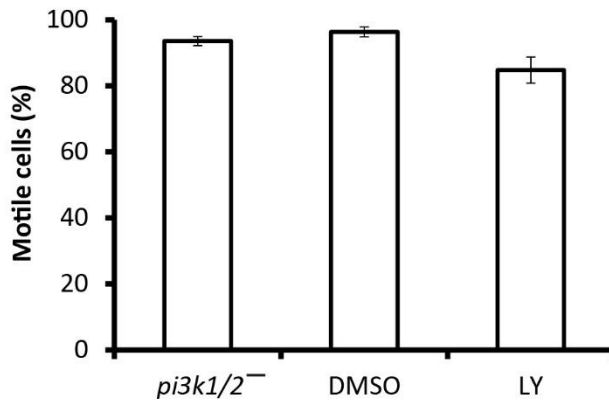


Fig. 1. Motility of wild-type KAx3 cells and *pi3k1/2* null cells in LY294002

(A) Motility of wild-type KAx3 cells was compared with those of the cells in the presence of LY294002 or DMSO. The percentage of motile cells were calculated from time-lapse recordings of EF-directed cell migration as described in Fig. 1. Motile cells were counted from the recordings and the number of motile cells were divided by that of total cells. (B) Motility of *pi3k1/2* null cells was compared with those of the cells in the presence of LY294002 or DMSO. Data are represented as mean \pm S.E.M. from three independent experiments.

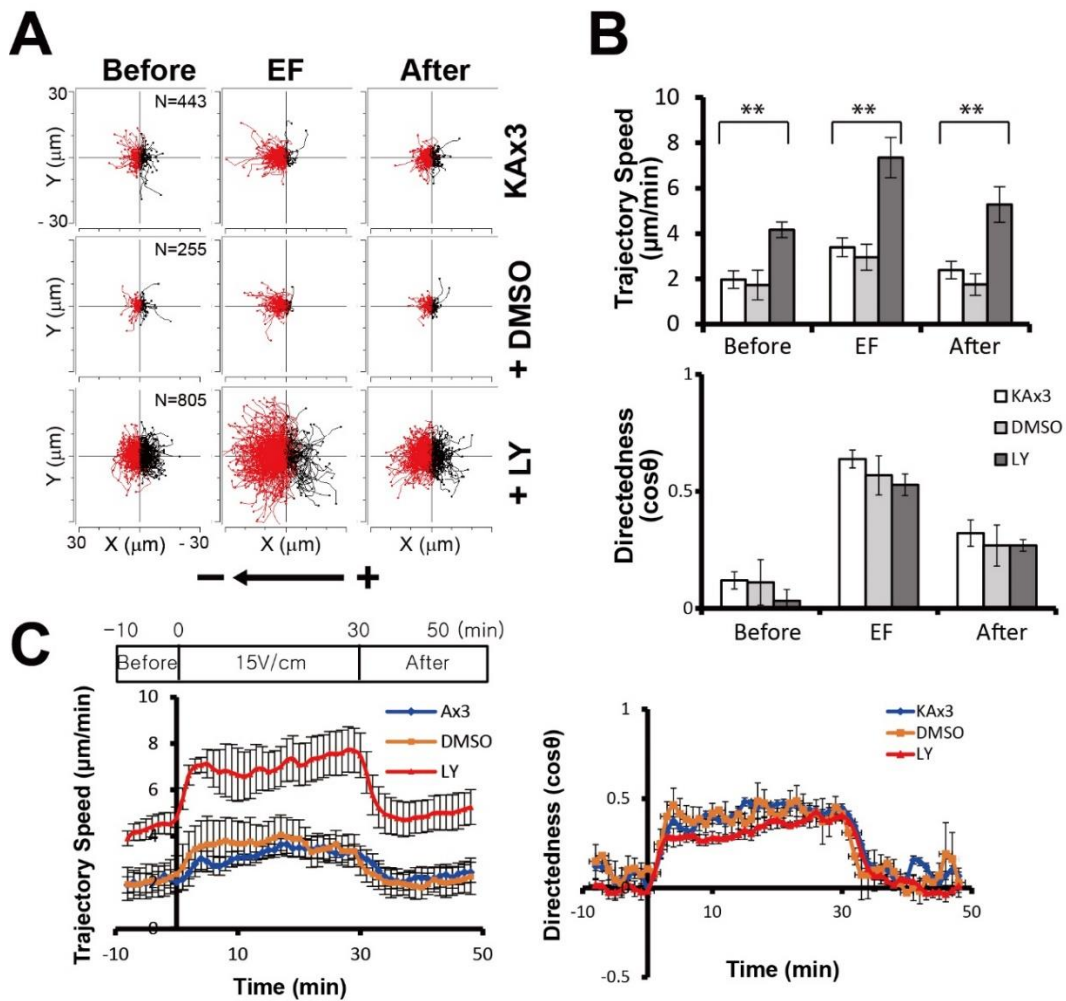


Fig. 2. (continued)

Fig. 2. Electrotactic responses of wild-type cells in the presence of LY294002

(A) Trajectories of wild-type KAx3 cells in an electric field (EF) of 15 V/cm. Trajectories of wild-type cells were compared with that of the cells in the presence of LY294002 (30 μ M) or DMSO (0.1 %) as a control. EF-directed cell migration was recorded at time-lapse intervals of 1 min for 60 min. EF of 15 V/cm was applied from the 10 to 40 min mark during recording. No EF was applied for the first 10 min and the last 20 min. “Before” indicates the period of time during the first 10 min without EF application. “EF” indicates the 10-min period after commencement of EF stimulation (20 to 30 min). “After” indicates the 10 min period after EF stimulation was stopped. Plots show migration paths of the cells with the start position of each cell centered at point 0,0. An arrow indicates the direction of the EFs. Cells migrate towards the cathode on the left in an EF. (B) Quantitative analyses of the directional migration of wild-type cells in an EF. Trajectory speed and directedness in the presence of LY294002 were compared with those of control cells in the absence of LY294002 or in the presence of DMSO. (C) Kinetics of trajectory speed and directedness in EF-induced directional migration. Trajectory speed and directedness were calculated every 2 min and sequentially plotted. Data are represented as mean \pm S.E.M. from three independent experiments with an EF of 15 V/cm. Statistical analysis was performed using the Student’s t-test, *P<0.05, **P<0.01.

III-2. Electrotaxis of *pi3k1/2* null cells in the presence of LY294002

To directly determine whether PI3K is involved in the regulation of cell motility in an inhibitory manner, I investigated the motility of *pi3k1/2* null cells in response to EF stimulation. As expected, based on the previous results, the *pi3k1/2* null cells were highly motile. Approximately 90 % of *pi3k1/2* null cells were motile, whereas only 20 % of wild-type cells displayed motility (Fig. 1B). When *pi3k1/2* null cells were treated with DMSO or LY294002, there was no significant difference in the percentage of motile cells compared with that of untreated *pi3k1/2* null cells. These findings are agreement with the previous data showing that inhibition of PI3Ks by LY294002 resulted in increased motility of 3 h starved cells.

Next, I examined the electrotactic responses of the *pi3k1/2* null cells. Before EF stimulation, *pi3k1/2* null cells were motile and showed approximately 2-fold higher motility than wild-type cells, similar to those of LY294002 treated cells. Upon EF stimulation, the elevated trajectory speed remained nearly constant (Fig. 3). There was no significant difference in directionality between the *pi3k1/2* null cells and wild-type cells. These data are similar to the results obtained while analyzing cell motility of wild-type cells in the presence of LY294002.

Six PI3Ks are present in *Dictyostelium* (Artemenko et al., 2014; Kolsch et al., 2008). To determine whether other PI3Ks are involved in the inhibition of cell motility, I examined the motility of *pi3k1/2* null cells in the presence of LY294002 (Fig. 3). The motility of *pi3k1/2* null cells in the presence of LY294002 was almost the same as that in the absence of LY294002. In addition, *pi3k1-5* null cells showed an elevated migration speed and normal directionality in response to EF stimulation similar to those observed in *pi3k1/2* null cells and wild-type cells in the presence of LY294002 (Fig. 4), suggesting that PI3K 1 and 2 play key roles in the regulation of cell motility. Taken together, these results support the assertion that PI3Ks play a suppressive role in cell motility of 3 h starved cells. The lack or inhibition of PI3K activity by LY294002 reverses the suppressive effect of PI3Ks on cell motility, leading to high motility.

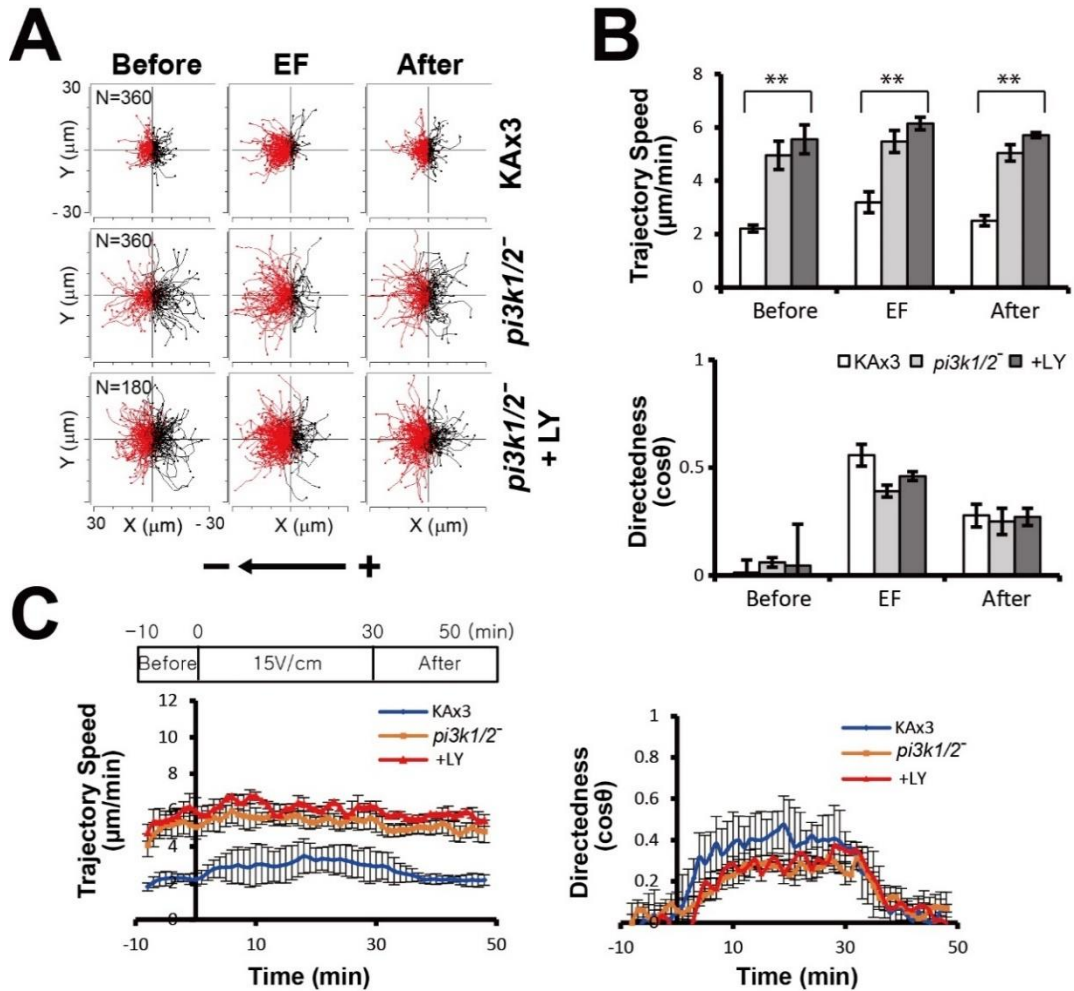


Fig. 3. Electrotactic responses of $pi3k1/2$ null cells in the presence of LY294002

(A) Trajectories of $pi3k1/2$ null cells in an EF of 15 V/cm. Trajectories of $pi3k1/2$ null cells in the presence or absence of LY294002 were compared with those of wild-type cells. (B) Quantitative analyses of the directional migration of $pi3k1/2$ null cells. (C) Kinetics of trajectory speed and directedness of $pi3k1/2$ null cells. Data are means \pm S.E.M. from three independent experiments in an EF of 15 V/cm. Statistical analysis was performed using the Student's t-test, * $P < 0.05$, ** $P < 0.01$

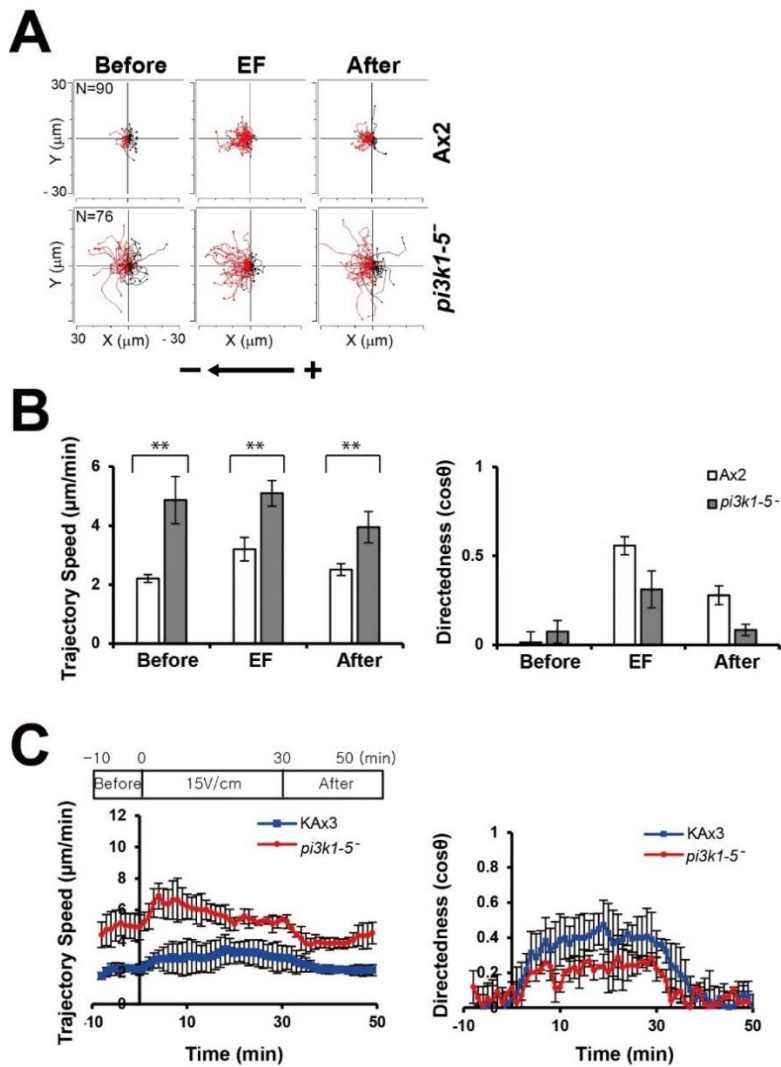


Fig. 4. Electrotactic responses of *pi3k1-5* null cells

(A) Trajectories of *pi3k1-5* null cells in an EF of 15 V/cm. Trajectories of *pi3k1-5* null cells in the presence or absence of LY294002 were compared with those of wild-type Ax2 cells. (B) Quantitative analyses of the directional migration of *pi3k1-5* null cells. (C) Kinetics of trajectory speed and directedness of *pi3k1-5* null cells. Data are means \pm S.E.M. from three independent experiments in an EF of 15 V/cm. Statistical analysis was performed using the Student's t-test, * $P < 0.05$, ** $P < 0.01$.

III-3. Random motility based on cell state in the presence of LY294002

PI3K is a key regulator of directional cell migration, especially chemotaxis. PI3K is required for directional cell migration in a shallow gradient of cAMP chemoattractants in *Dictyostelium* (Funamoto et al., 2002; Kolsch et al., 2008). In chemotaxis assay using *Dictyostelium*, the cells should be first aggregation competent by pulsing with the chemoattractant cAMP at 6 min intervals for 5~6 h. Under these conditions, several studies have reported that lack of PI3K or inhibition of PI3K with LY294002 results in a decrease in cell motility (Funamoto et al., 2002; Loovers et al., 2006; Sasaki et al., 2004), which is contrary to the results observed in my current experiments using 3 h starved cells.

To determine which experimental conditions (usage of aggregation-competent cells or 3 h starved cells) caused the discrepancy in the effects exerted by PI3Ks on cell motility, I examined and compared random motilities expressed under these two conditions; 3 h starvation (vegetative) and 6 h pulsing of the cells with cAMP (aggregation-competent). First, I compared the random motilities among the wild-type cells under these two conditions (Fig. 5). Wild-type Ax3 showed approximately 2.2 $\mu\text{m}/\text{min}$ motility under 3 h starvation. As previously observed while analyzing electrotaxis (Fig. 2), the trajectory speed of wild-type cells after 3 h of starvation increased in the presence of LY294002 to 4.2 $\mu\text{m}/\text{min}$. When the cells became aggregation competent on pulsing with cAMP for 6 h, the trajectory speed increased to approximately 6.5 $\mu\text{m}/\text{min}$ as expected of aggregation-competent cells. Interestingly, treatment of aggregation-competent cells with LY294002 resulted in a decrease in the migration speed from 6.5 $\mu\text{m}/\text{min}$ to 4.1 $\mu\text{m}/\text{min}$. These data indicate that the effects of LY294002 on cell motility differ depending on the state of the cells; LY294002 promotes motility in 3 h starved cells while suppressing the same in aggregation-competent cells. These results also suggest that PI3K plays an inhibitory role in regulating cell motility in 3 h starved cells, whereas it plays a stimulatory role in aggregation-competent cells.

To investigate the role of PI3K in cell motility, I examined the motilities of *pi3k1/2* null cells under both conditions. *pi3k1/2* null cells had higher migration speed (4.2 $\mu\text{m}/\text{min}$) than wild-type cells (2.2 $\mu\text{m}/\text{min}$) after 3 h starvation, and the motility increased slightly to 6.1 $\mu\text{m}/\text{min}$ in the presence of LY294002 (Fig. 6). Aggregation-competent *pi3k1/2* null cells displayed similar results as the wild-type cells – they exhibited high motility compared with that of 3 h starved cells. However, contrary to the results observed in 3 h starved cells, the trajectory speed of *pi3k1/2* null cells did not increase but rather decreased to 6.3 $\mu\text{m}/\text{min}$ in the presence of LY294002. These results support the assertion that PI3K suppresses the motility of 3 h starved cells while promoting the motility of aggregation-competent cells.

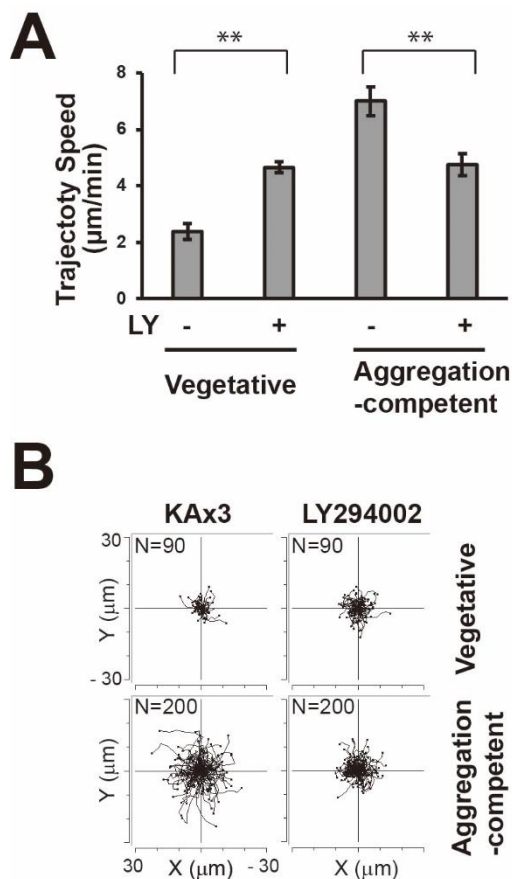


Fig. 5. Random motility of wild-type cells on the vegetative or the aggregation-competent conditions

(A) Trajectory speed of wild-type cells in random migration. Trajectory speeds of wild-type cells on the vegetative and the aggregation competent conditions were compared. In addition, random motility of the cells on each condition were compared with those in the presence of LY294002 (30 μM). Data are means ± S.E.M. from three independent experiments and statistical analysis was performed using the Student's t-test, *P<0.05, **P<0.01. (B) Trajectories of the cells in random migration. Plots show migration paths of the cells with the start position of each cell centered at point 0,0.

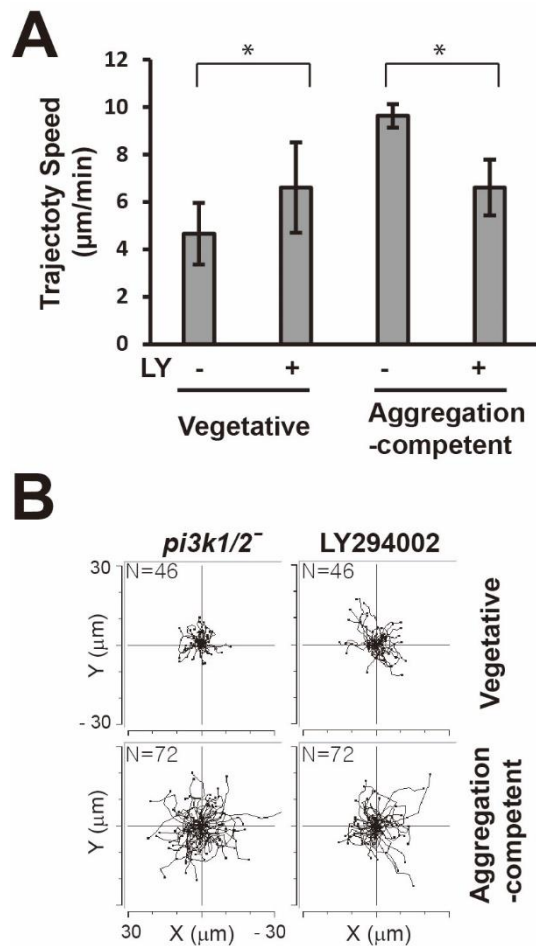


Fig. 6. Random motility of *pi3k1/2* null cells on the vegetative or the aggregation-competent conditions

(A) Trajectory speed of *pi3k1/2* null cells in random migration. Trajectory speeds of *pi3k1/2* null cells on the vegetative and the aggregation competent conditions were compared. In addition, random motility of the cells on each condition were compared with those in the presence of LY294002 (30 µM). Data are means ± S.E.M. from three independent experiments and statistical analysis was performed using the Student's t-test, *P<0.05, **P<0.01. (B) Trajectories of the cells in random migration. Plots show migration paths of the cells with the start position of each cell centered at point 0,0.

IV. DISCUSSION

In this study, I aimed to investigate the roles of PI3K in directional cell migration in EF and found that their roles differ depending on the vegetative, and aggregation-competent states of the cells. It appears that PI3K plays a suppressive role in regulating the motility of vegetative cells, whereas it plays a promotive role in the motility of aggregation-competent cells. Cell migration studies using *Dictyostelium*, a well-developed model organism, have focused on chemotaxis, and most of important signaling molecules involved in directional cell migration have been identified and characterized in chemoattractant-mediated cell migration studies (Artemenko et al., 2014; Kolsch et al., 2008; Lee and Jeon, 2012a). To study chemotaxis using cAMP as a chemoattractant, *Dictyostelium* cells must first become aggregation-competent by pulsing with cAMP at a constant interval for 5~6 h, as vegetative cells are insensitive to the chemoattractant cAMP (Artemenko et al., 2014; Funamoto et al., 2002; Jeon et al., 2007). *Dictyostelium* has a unique life cycle. During abundant nutrient availability in the media, they live in a single-cell state (vegetative). In contrast, when the cells are starved, *Dictyostelium* cells undergo a series of developmental processes within a day to form multicellular structures - a mound, a slug, and finally a fruiting body. To form an aggregate multicellular structure, cells secrete cAMP chemoattractant into their surroundings, express signaling molecules responding to cAMP, and then become aggregation-competent around an aggregation center (Chisholm and Firtel, 2004a; Siu et al., 2011). Under these conditions, PI3Ks play important roles in directional sensing and creating a positive feedback loop for F-actin polymerization and protrusions at the front of the cell (Kolsch et al., 2008; Sasaki et al., 2004). Many studies have reported that cells in the presence of LY294002, a PI3K inhibitor, as well as *pi3k* null cells show decreased migration speed compared with that of wild-type cells (Funamoto et al., 2002; Loovers et al., 2006; Sasaki et al., 2004). my data are in agreement with previously reported results, indicating that PI3K plays a positive role in cell motility in the aggregation-competent state.

PI3K and Akt/Pkb signaling pathways are activated on a direct EF and are required for directional cell migration and wound healing in mammalian cells (Zhao et al., 2006). However, the roles of PI3Ks in electrotaxis have not yet been studied using *Dictyostelium* model organism. Unexpectedly, I found that treatment with LY294002 increased cell motility rather than decrease it as was expected based on the results of chemotaxis studies both with and without EF application. I posit that these unexpected observations resulted from the difference in the experimental conditions between chemotaxis and electrotaxis. *Dictyostelium* shows strong electrotaxis and moved towards the cathode upon EF stimulation. In contrast to chemotaxis, *Dictyostelium* cells display strong electrotaxis in various developmental stages, including vegetative, 3-h starved, and aggregation-competent states (Gao et al., 2015b; Jeon et al., 2019; Zhao, 2009b). Cells lacking G-protein coupled receptors or G proteins, which are essential for chemotaxis towards cAMP, respond well to an EF and show directional movements (Zhao, 2009b; Zhao et al., 2002). Earlier, aggregation-competent cells were used in the study of electrotaxis as in chemotaxis (Gao et al., 2011; Sato et al., 2009; Zhao et al., 2002). However, 3-h starved *Dictyostelium* cells have been used recently in the study of directional cell migration in response to an EF (Gao et al., 2015b; Jeon et al., 2019). In the present study, I first examined cell motility under the condition of 3-h starvation. Unexpectedly, most of the wild-type cells that were non-motile became highly motile in the presence of the PI3K inhibitor LY294002. The 3 h starved vegetative cells showed increased motility following treatment with LY294002, whereas aggregation-competent cells exhibited slightly decreased motility. Similarly, compared with wild-type cells, *pi3k* null cells in the vegetative state showed increased motility. These results are supported by random migration experiments. It is likely that cell motility in the vegetative state is suppressed by PI3Ks, and this suppression is reversed by inhibition or lack of PI3Ks.

Usually, cell motility increases with the progression of the developmental stages (Artemenko et al., 2014; Chisholm and Firtel, 2004a; Guido et al., 2020; Siu et al., 2011). Compared with vegetative cells, aggregation-competent cells have increased motility. It has been suggested that cells secrete signaling molecules to induce cell motility and electrical sensing in response to the

external EF when they begin to starve (Guido et al., 2020). These molecules would have been involved in coordinating cell migration to promote aggregation by regulating cAMP signal transduction, such as activation of Ca^{2+} influx, activation of adenylyl cyclases, guanyl cyclases, and cGMP signaling (Clarke and Gomer, 1995; Yuen et al., 1995). my results suggest that PI3K does play a role in regulating cell motility during the various development phases in *Dictyostelium*. However, the mechanism underlying the suppression of motility in vegetative cells due to the inhibition or removal of PI3Ks is still unknown. Exploring the relationship between PI3K-mediated lipid signaling and cAMP/cGMP signaling would aid in understanding the regulation of cell motility during the progression of the developmental stages in *Dictyostelium*.

This part has been published as Wonbum Kim and Taeck J. Jeon, 2023

PART II. Dynamic subcellular localization of DydA in

***Dictyostelium* cells**

I. INTRODUCTION

Cell migration is a coordinated process in which the leading edge of a cell extrudes a pseudopod or lamellipod in the direction of the chemoattractant and is mediated by localized F-actin polymerization. Myosin II-mediated contraction of the cell's posterior is coordinated with the leading-edge protrusions. For a cell to migrate in the direction of a chemoattractant source, it first detects the chemoattractant gradients through membrane-bound receptors and converts the extracellular signal to localized intracellular signals through several signaling pathways (Artemenko et al., 2014; Kolsch et al., 2008; Kortholt and van Haastert, 2008). Ras activation is the earliest response to chemoattractant stimulation and occurs downstream of receptors and heterotrimeric G proteins (Kortholt and van Haastert, 2008).

Ras proteins are small monomeric GTPases that act as crucial regulators of several cellular signaling pathways, including proliferation, cytoskeletal function, chemotaxis, differentiation and apoptosis. The Ras GTPase subfamily consists of 15 proteins including 11 Ras, three Rap, and one Rheb related proteins in *Dictyostelium*. RasC, RasG, and RapA are activated in response to cAMP chemoattractant stimulation and control cell motility. Activated Ras proteins are enriched at the leading edge of chemotaxing cells, where they locally activate signaling molecules, including phosphatidylinositol 3-kinase (PI3K) and target of rapamycin complex 2 (TORC2) (Artemenko et al., 2014; Kolsch et al., 2008; Kortholt and van Haastert, 2008; Lee and Jeon, 2012a).

Daydreamer (DydA), a member of the Mig10/RIAM/lamellipodin (MRL) family of adaptor proteins, is a downstream effector of RasG. DydA localizes at the leading edge of migrating cells and is required for directional sensing and cell polarization during chemotaxis. DydA is involved

in the negative regulation of the PI3K signaling pathway in controlling F-actin and myosin II assembly in response to chemotactic stimulation (Kölsch et al., 2013). DydA is phosphorylated by glycogen synthase kinase-3 (GSK-3), and this phosphorylation is associated with the function of DydA in the regulation of PKB, PKBR1, and MyoII assembly (Romero et al., 2018). DydA contains several domains that affect its subcellular localization, including two Ras-associating (RA) domains, a pleckstrin homology (PH) domain, a proline-rich motif (PRM), and two calponin homology (CH) domains. Here, I examined the dynamic subcellular localizations of a series of truncated DydA proteins, and characterized each domain affecting DydA localization in response to chemoattractant stimulation.

II. MATERIALS AND METHODS

II-1. Strains and plasmids

Dictyostelium wild-type KAx3 cells were cultured axenically in HL5 medium at 22 °C. For expression of GFP-DydA, the full coding sequence of DydA cDNA was generated by RT-PCR with two primers containing a *Bam*HI and a *Xho*I site at the end of the primers, respectively. Full-length DydA was digested with *Bam*HI/*Xho*I restriction enzymes and cloned into the *Bgl*III-*Xho*I site of the expression vector pEXP-4(+) containing a GFP fragment (Jeon, 2007). The full coding sequence of DydA was confirmed by sequencing and transformed into KAx3 wild-type cells. For expression of the truncated DydA proteins, the regions in DydA marked in the diagram (Fig. 2A and Fig. 3B) were amplified by PCR as in constructing full-length GFP-DydA and cloned into the *Bgl*III-*Xho*I site of a pEXP4(+) vector containing a GFP fragment. The expression plasmids for GFP-ABP and RFP-coronin have been previously described (Jeon, 2007; Kim et al., 2017; Lee et al., 2014). The plasmids were transformed into KAx3 cells, and the cells were maintained in 20 mg/ml of G418, 50 mg/ml of hygromycin, or both as required.

II-2. Chemotaxis and image acquisition

The subcellular localization of GFP-fusion proteins upon chemoattractant stimulation was investigated as previously described (Jeon, 2007; Kim et al., 2017; Lee et al., 2014). To prepare aggregation-competent cells for the study, vegetative cells were washed twice with Na/K phosphate buffer, then resuspended in the same buffer at a density of 5×10^6 cells/ml, and pulsed with 30 nM cAMP at 6-min intervals for 5 h. The aggregation-competent cells were then seed in glass-bottomed microwell plates. To image the chemotaxing cells, a micropipette containing 150 mM cAMP was placed near the cells for stimulation. Images of the chemotaxing cells were captured at time-lapse intervals of 6 s for 30 min using an inverted microscope (IX71; Olympus, Japan) equipped with a camera (DS-Fi1; Nikon, Japan).

II-3. Quantitative analysis of membranes

To quantify the membrane or cortical localization of GFP fusion proteins, the intensity of the fluorescence in response to chemoattractant stimulation was measured as previously described (Jeon, 2007; Kim et al., 2017; Lee et al., 2014). Aggregation-competent cells were allowed to adhere to plates for 10 min and then were uniformly stimulated with a final concentration of 10 mM cAMP by pipetting 200 μ l of 150 mM cAMP into a plate containing 3 ml of cells. Fluorescence images were captured at time-lapse intervals of 1 s for 1 min using an inverted microscope. The NIS-elements software from Nikon was used to capture the frames, and ImageJ software from the National Institutes of Health (USA) was utilized to analyze them. I measured the fluorescence intensity in the cell cortex and determined the level of cortical GFP by dividing the intensity at each time point (E_t) by the intensity before stimulation (E_o).

III. RESULTS

III-1. Domain structure of DydA and localization of DydA

DydA encodes 1211 amino acids and contains two RA domains at its N- and C- termini, a pleckstrin homology (PH) domain, and two calponin homology (CH) domains. DydA also contains a prolin-rich motif (PRM) in the middle of the protein (Fig. 1A). No protein showing significant homology was detected when the full-length DydA amino acid sequence was used in the BLAST search. However, the domain structure of DydA is similar to that of the MRL (Mig10/RIAM/Lpd) family proteins, such as RIAM and Lamellipodin (Krause et al., 2004; Lafuente et al., 2004), all of which have a consecutively arranged RA and PH domains as well as a PRM. DydA has a PRM behind the RA and PH domains and an additional RA domain in the C-terminus, whereas RIAM and Lamellipodin, which are the MRL family proteins, contain a PRM followed by RA and PH domains. I used a GFP-DydA fusion protein to examine the subcellular localization of DydA protein in cells (Fig. 1B). In vegetative cells, GFP-DydA was found in the cytosol and accumulated at the regions of membrane ruffling and macropinosomes, where F-actin and phosphatidylinositol (3,4,5)-trisphosphate (PIP3) accumulate (Kolsch et al., 2008). To determine the temporal and spatial dynamic localization of DydA in response to cAMP chemoattractants, aggregation competent cells were prepared by pulsing cells with cAMP for 5 h and examined the translocation kinetics of GFP-DydA in response to uniform chemoattractant stimulation (Fig. 1D). Before chemoattractant stimulation, GFP-DydA was detected in the cytosol. Upon stimulation, DydA translocated rapidly and transiently to the cell cortex. Quantification of fluorescence in the cell cortex indicated the translocation of DydA in the cytosol to the cell cortex with a peak at 6~8 s after stimulation (Fig. 1E). In cells moving up a chemoattractant gradient, GFP-DydA was spatially localized to the leading edge, suggesting that DydA plays a role in the anterior region of a moving cell in response to chemoattractant stimulation.

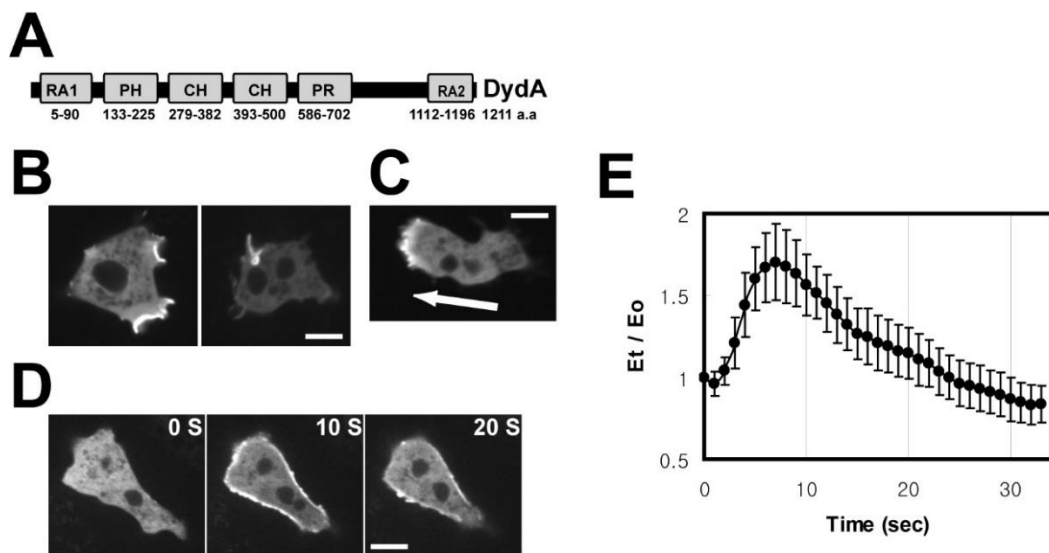


Fig. 1. Domain structure and localization of full-length DydA

(A) Domain structure of full-length DydA. (B) Localization of GFP-DydA. Cells expressing GFP-DydA in the vegetative cells were imaged. Scale bar, 5 μ m. (C) GFP-DydA in migrating aggregation-competent cells was imaged. The arrow indicates the direction of moving cells. (D) Translocation of GFP-DydA to the cell cortex in response to uniform chemoattractant stimulation. Aggregation-competent cells were stimulated with cAMP and the time-lapse images were recorded. The representative images at 0, 10, 20 s after stimulation are presented. Scale bar, 5 μ m. (E) Translocation kinetics of GFP-DydA to the cell cortex in response to chemoattractant stimulation. Fluorescence intensity at the cell cortex was quantified as described previously. Data are presented as means \pm SD from three separate experiments.

III-2. Characterization of the domains of DydA for localization

To determine which domains are responsible for the localization of DydA in response to chemoattractant stimulation, I prepared a series of GFP-fusion truncated DydA proteins and examined the temporal localization of these proteins in response to chemoattractant stimulation and the spatial localization in moving cells (Fig. 2). GFP-RA1, which contains the RA domain at the N-terminus, was observed in the anterior region of chemotaxing cells and was rapidly and transiently translocated to the cell cortex in response to chemoattractant stimulation (Fig. 2B), as GFP-DydA containing full-length DydA did. Quantification of the fluorescence of the proteins showed the translocation of GFP-RA1 to the cell cortex with a peak at 4~6 s after stimulation, which was 2~3 s earlier than that of GFP-DydA (Fig. 2C). These results suggest that there are additional regions to affect DydA localization. In contrast, GFP-PH and GFP-CH proteins, despite possessing the RA1 domain, showed only slight translocation to the cell cortex upon chemoattractant stimulation. During chemotaxis, these proteins were evenly distributed without clear localized accumulation at the anterior of the moving cells. Interestingly, GFP-PRMA containing all the domains, RA1, PH, CH, and PRM, displayed similar localization in chemotaxing cells and translocation upon chemoattractant stimulation as those of GFP-RA1 and GFP-DydA (Fig. 2B). The translocation kinetics of GFP-PRMA with a peak at 5~7 s was similar to those of GFP-DydA, 2~3 s later than those of GFP-RA1 (Fig. 2C). These results suggest that both the RA1 domain and the PRM region play a role in controlling protein localization. The PH and CH domains are unlikely to regulate DydA localization. Instead, domains such as PH and CH seems to interfere with the localization of DydA via the RA1 domain and the PRM region. GFP-RA2, containing the RA domain at the C-terminus, was evenly distributed in the cytosol of chemotaxing cells and showed no translocation to the cell cortex upon chemoattractant stimulation. In contrast to RA1, the RA2 domain appears to be dispensable for controlling DydA localization in response to chemoattractant stimulation. GFP-PRMB, containing both the RA2 domain and the PRM region, showed clear translocation to the cell cortex upon stimulation and

was found in the anterior region of migrating cells (Fig. 2B and C), supporting the idea that the PRM region is required for the translocation of the protein to the cell cortex upon stimulation and preferential localization at the leading edge of migrating cells. To determine whether the PRM alone is sufficient for translocation to the cortex and differential localization at the front of moving cells, I examined the localization of GFP-PRM, which contains only the PRM region (Fig. 2A). GFP-PRM translocated to the cell cortex with a peak at 6~8 s similar to GFP-DydA, and was located at the leading edge of the migrating cells (Fig. 2B and C). These results indicate that both the RA1 domain and the PRM region mediate the translocation of DydA proteins to the cell cortex upon chemoattractant stimulation and differential localization at the anterior region of migrating cells. The translocation kinetics of these proteins suggest that the PRM region plays a dominant role in controlling the localization of DydA.

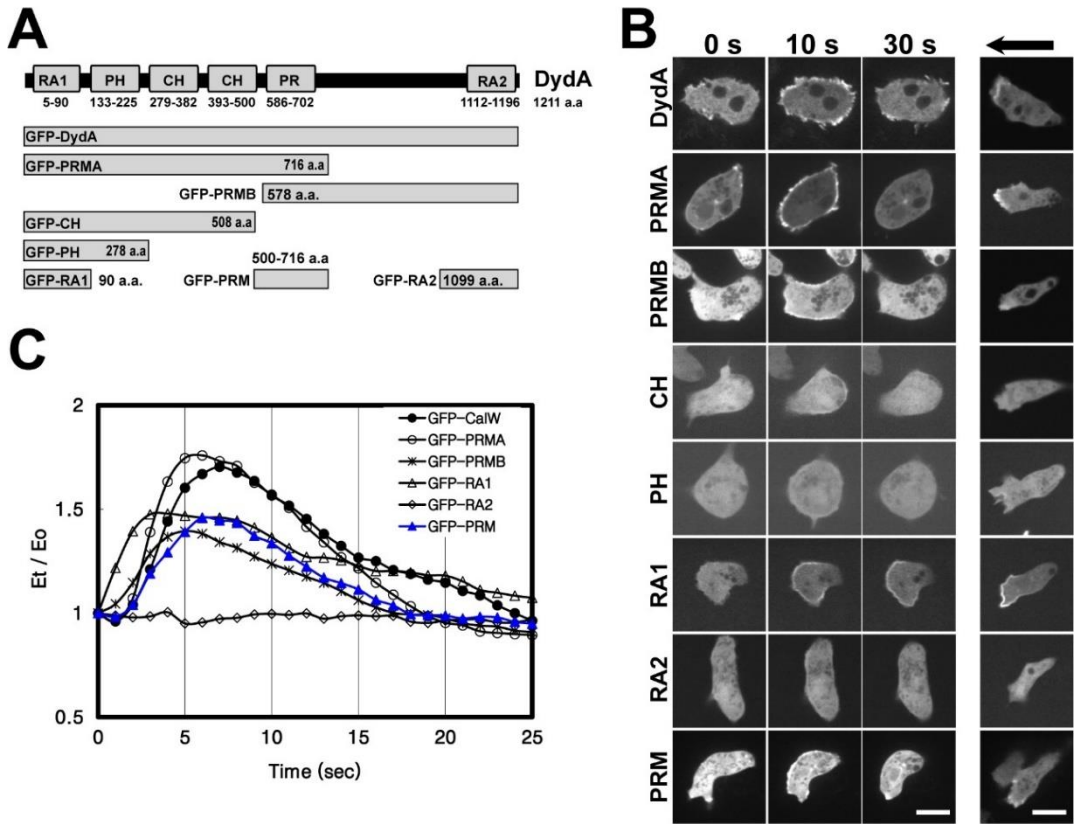


Fig. 2. Localization of truncated DydA proteins

(A) Domain structure of DydA and schematic diagram of truncated DydA proteins. (B) Localization of truncated GFP-DydA proteins. Translocation of truncated DydA proteins to the cell cortex in response to chemoattractant stimulation (left). Cells expressing truncated GFP-DydA proteins were uniformly stimulated with cAMP and time-lapse images were recorded. Representative images at 0, 10, 30 s after stimulation are presented. Localization of the truncated proteins in migrating cells (right). The arrow indicates the direction of movement. Scale bar, 5 μ m. (C) Translocation kinetics of truncated GFP-DydA proteins to the cell cortex in response to uniform cAMP stimulation. Fluorescence intensity at the cell cortex was quantified as previously described. Graphs are the means of several cells from time-lapse recordings from at least three separate experiments.

III-3. Actin foci localization of DydA

DydA negatively regulates actin cytoskeleton. *dydA* null cells have elevated F-actin level and defects in polarization and in regulating actin cytoskeleton. Microscopic examination of *dydA* null cells showed numerous F-actin-enriched microspikes (filopodia), which appeared as spiny projections from the surface of the cells, suggesting aberrant organization of the actin cytoskeleton (Kölsch et al., 2013). GFP-Abp, which binds to F-actin and is used to localize F-actin in vivo (Westphal et al., 1997), was localized at the projections in the cells (Fig. 3A), indicating that the pointed projections are F-actin enriched structures. In addition, GFP-Abp was detected at the foci at the bottom of the cells. Actin foci have been suggested to function as active feet of cells (Uchida and Yumura, 2004). Interestingly, GFP-DydA was detected in the foci at the bottom of the cells (Fig. 3A). To determine the region required for localization to the actin foci, I examined the bottom of cells expressing a series of truncated DydA proteins (Fig. 3B). Only truncated DydAs containing the PRM region, such as GFP-DydA, GFP-PRMA, and GFP-PRMB, displayed actin foci at the bottom of the cells (Fig. 3B), but not other proteins that did not include the PRM region, such as GFP-RA1, GFP-PH, GFP-CH, and GFP-RA2 (data not shown). GFP-PRM, which contained only the PRM region, exhibited actin foci at the bottom of the cells, indicating that the PRM region was essential and sufficient for the localization of DydA to the actin foci at the bottom of the cells.

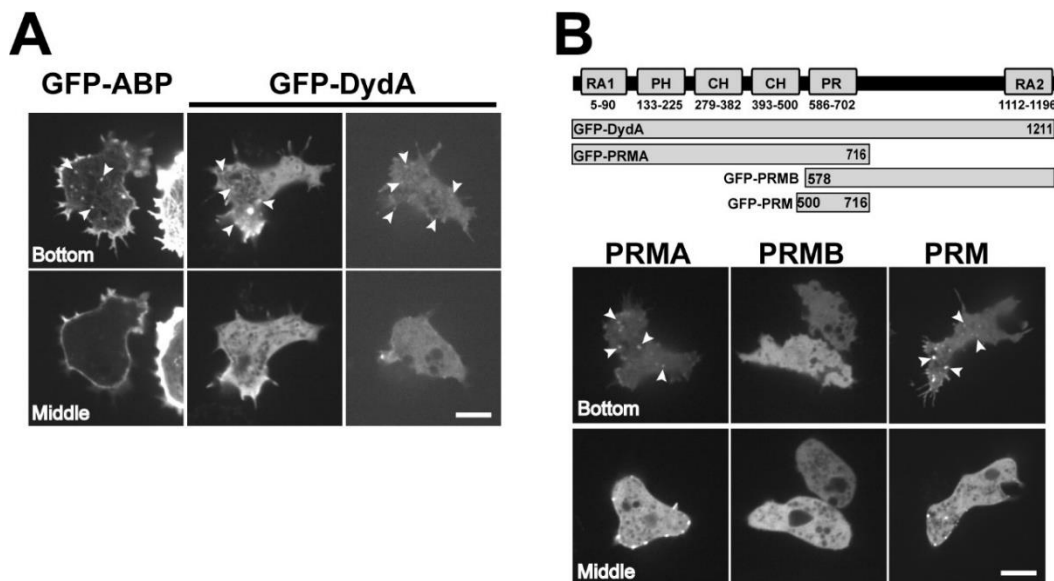


Fig. 3. Actin foci localization of DydA

(A) Actin foci at the bottom of cells expressing GFP-DydA or GFP-ABP. Bottom or middle sections of cells were imaged with a confocal microscope. Arrow heads indicates foci at the bottom of cells. Scale bar, 5 μ m. (B) Actin foci at the bottom of cells expressing the PRM region of DydA. Domain structure of DydA and truncated DydA containing the PRM region (upper panel). Bottom or middle sections of cells expressing truncated DydA containing the PRM region were imaged. Arrow head indicates actin foci at the bottom of cells. Scale bar, 5 μ m.

III-4. Colocalization of GFP-PRM and RFP-coronin

To confirm whether the foci displayed by GFP-DydA coincided with the actin foci displayed by GFP-Abp, I prepared cells expressing both GFP-PRM and RFP-coronin and examined the colocalization of the two proteins (Fig. 4). Coronin is an actin-binding protein required for efficient cell protrusion and migration. Coronin is used as a marker protein for newly formed F-actin and to study the localization of the dynamic F-actin-rich areas of cells (Humphries et al., 2002; Jeon, 2007; Rodal et al., 2005). I attempted to co-express both GFP-DydA and RFP-coronin, but failed. The expression level of GFP-DydA was too low for further analysis. Both GFP-PRM and RFP-coronin were localized to the same leading edge of the migrating cells and were transiently translocated to the cell cortex in response to chemoattractant stimulation (Fig. 4A). Translocation kinetics showed that the response of GFP-PRM occurred 2~3 s earlier than that of RFP-coronin. GFP-PRM displayed a translocation peak at 6~8 s after stimulation, whereas RFP-coronin exhibited a peak at 9~11 s after stimulation (Fig. 4B and C).

When I examined the bottom of the cells, both GFP-PRM and RFP-coronin were detected at the foci (Fig. 4D). The sites of the actin foci displayed by GFP-PRM and RFP-coronin were the same; however, the time of appearance differed slightly. In the first panel of Fig. 4D, no foci were observed at the site indicated by the arrowhead. In the second panel (image at 7 s in the recording), only GFP-PRM appears at the site indicated by the arrowhead, but not RFP-coronin. In the third and fourth panels (images at 9 s and 14 s), both GFP-PRM and RFP-coronin are shown at the site, indicating that GFP-PRM appears 2 s earlier than RFP-coronin. In the fifth panel (image at 20 s), GFP-PRM disappears after approximately 13 s, but RFP-coronin still exists. In the sixth panel (image at 23 s), RFP-coronin disappears. These results indicate that GFP-PRM not only appears but also disappears 2 s earlier than RFP-coronin. The duration of GFP-PRM and RFP-coronin were similar at 13~14 s (Fig. 4D). These results agree with the translocation kinetics of GFP-PRM and RFP-coronin, in which GFP-PRM preceded RFP-coronin by 2~3 s in response to uniform chemoattractant stimulation.

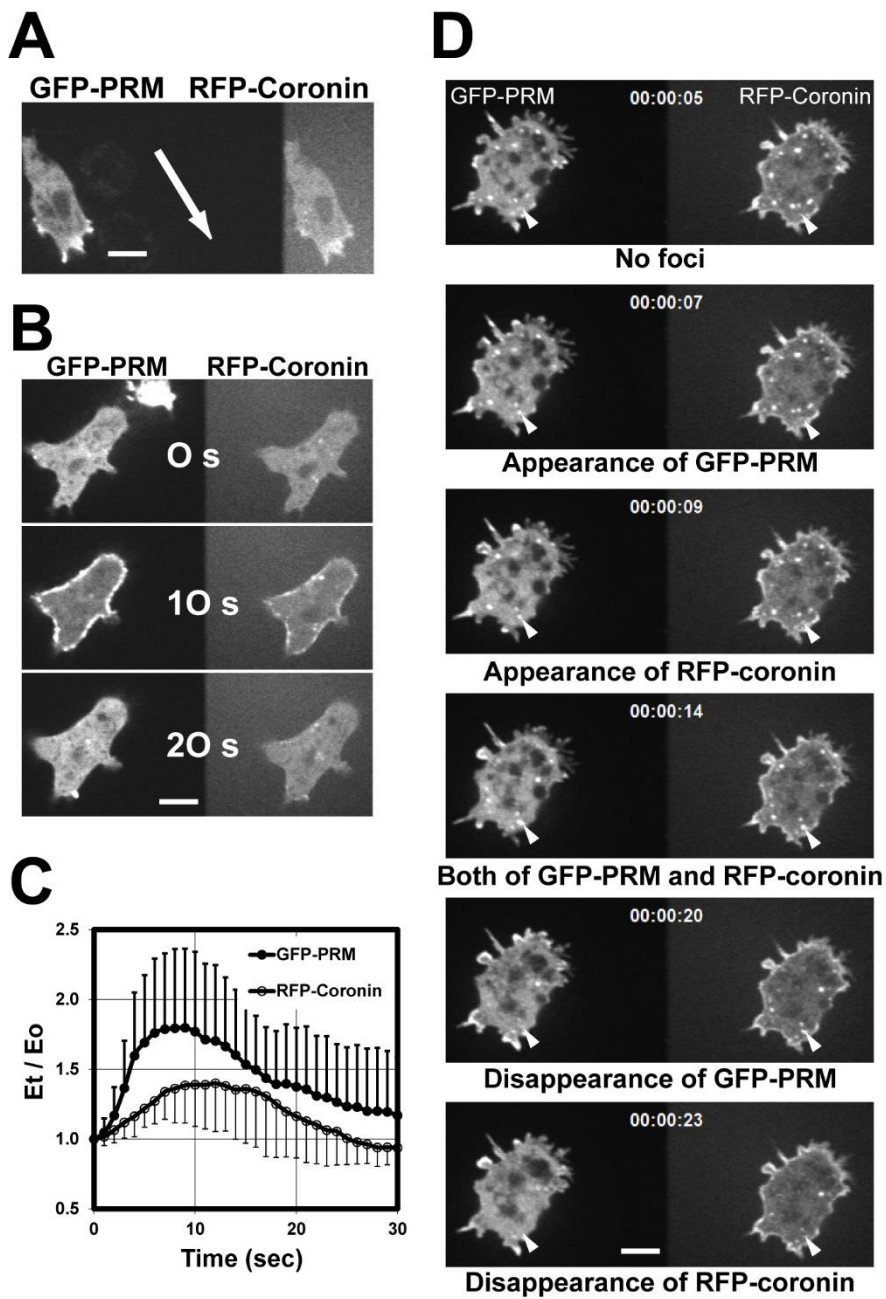


Fig. 4. (continued)

Fig. 4. Colocalization of the PRM region and coronin Dual-view analyses of cells expressing both GFP-PRM and RFP-coronin, which is a marker protein for newly formed F-actin

(A) Localization of the proteins in migrating cells. The arrow indicates the direction of moving cells. Scale bar, 5 μm . (B) Translocation of the proteins to the cell cortex in response to chemoattractant stimulation. The representative images at 0, 10, 20 s after stimulation from time-lapse recordings are presented. Scale bar, 5 μm . (C) Translocation kinetics of the proteins to the cells cortex in response to uniform chemoattractant stimulation. Fluorescence intensity at the cell cortex was quantified as previously described. Data are presented as means \pm SD from several cells of at least three separate experiments. (D) Dynamics of actin foci at the bottoms of cells expressing GFP-PRM and RFP-coronin. Bottom images of cells were recorded and analyzed at various time points, as indicated. No actin foci were found at the site indicated by the arrowhead in the first panel at 5 s. Sequentially GFP-PRM and RFP-coronin appear at the foci at 7 s and 9 s, respectively. In the fifth and sixth panel, two proteins disappear at the actin foci at 20 s and 23 s, respectively. Scale bar, 5 μm .

IV. DISCUSSION

My results demonstrate that DydA localizes to the cell cortex and actin foci at the bottom of cells through the PRM region of DydA. DydA contains several domains, including an RA domain in the N-terminal region, a PH domain, two CH domains, and a PRM region in the central region. Here, I characterized the domains that affect the localization of DydA and found that the RA1 domain at the N-terminus and the PRM region were responsible for the translocation of DydA to the cell cortex upon chemoattractant stimulation and differential localization at the leading edge of chemotaxing cells. The localization of DydA to the actin foci at the bottom of cells was mediated by the PRM region. The PRM was sufficient for the localization of DydA at actin foci. The translocation kinetics to the cell cortex in response to uniform chemoattractant stimulation showed that the response of PRM was 2~3 s faster than that of coronin, which is an actin binding protein that plays an inhibitory role in F-actin assembly (Humphries et al., 2002). In accordance with these results, the appearance and disappearance of GFP-PRM at the actin foci at the bottom of the cells was 2~3 s earlier than that of coronin. These results suggest that the PRM region plays an important role in relaying signals from the upstream regulator RasG proteins to downstream effectors, such as PI3Ks and Akt/PKB proteins, by mediating the localization of DydA to the cell cortex in response to chemoattractant stimulation.

DydA is involved in actin cytoskeleton reorganization. Cells lacking DydA are significantly less polarized than wild-type cells and move more slowly toward the cAMP source, with significantly decreased migration speed and directionality (Kölsch et al., 2013). *dydA* null cells display numerous microspikes around the cell surface and elevated levels of F-actin compared to wild-type cells. DydA has been suggested to play an inhibitory role in F-actin assembly (Kölsch et al., 2013; Romero et al., 2018). In support of the cytoskeletal role of DydA, GFP-fusion DydA localizes to the cell cortex in response to chemoattractant stimulation. The localization and translocation kinetics of DydA to the cell cortex upon stimulation are similar to those of activated RasG, PKB, and many other proteins involved in cytoskeletal reorganization,

such as Arp2/3 and coronin proteins (Jeon, 2007; Kortholt and van Haastert, 2008; Sasaki et al., 2004; Sasaki and Firtel, 2006). The present study showed that the RA1 domain and the PRM region, among several domains in DydA, play a role in recruiting DydA to the site of F-actin assembly, including the anterior region of migrating cells and actin foci at the bottom. The actin cytoskeleton allows the cells to control their shape and motility. The domain structure of DydA is similar to that of the MRL (Mig-10/RIAM/Lpd) family proteins (Krause et al., 2004; Lafuente et al., 2004). Among the MRL family proteins, RIAM interacts with Rap1, a Ras protein, and links Rap1 to cell adhesion by regulating actin dynamics (Krause et al., 2004; Lafuente et al., 2004). My results suggest that DydA links RasG, an upstream regulator of DydA, to the regulation of actin cytoskeleton through the PRM region, ultimately affecting cell morphology and migration.

Proline-rich sequences, which play a crucial role in mediating a wide range of protein-protein interactions, are found throughout both prokaryotes and eukaryotes (Li, 2005; Ravi Chandra et al., 2004). The polyproline type II (PPII) helix, which has three residues per turn is left-handed, is the most common structure formed by two or more proline residues in a row (Li, 2005; Schweimer et al., 2002). Protein domains that recognize the proline-rich sequences include the SH3 domain, the WW domain, the EVH1 [Enabled/VASP (vasodilator-stimulated protein) homology] domain, and profilin (Li, 2005). The EVH1 domain and profilin have been implicated in actin cytoskeletal rearrangements (Mahoney et al., 1999; Prehoda et al., 1999). DydA is involved in cytoskeletal reorganization. Identifying the binding partner of DydA through the PRM region will greatly contribute to understanding the mechanisms for relaying signals from Ras signaling to downstream effectors such as PI3Ks, Akt/Pkb, and ultimately the actin cytoskeleton.

PART III. Role of Shaker-like potassium channels in cell migration in *Dictyostelium*

I. INTRODUCTION

Various external stimuli can induce directed cell migration. Electrotaxis, which is directional cell migration in an electric field (EF), is involved in a wide range of physiological processes, such as embryogenesis, neuronal guidance, wound healing, and metastasis (Gao et al., 2015a; Tai et al., 2018; Zhao, 2009a). The molecular mechanism of directional cell migration is primarily based on chemoattractant-directed cell migration. At the cell surface, G-protein coupled receptors transmit external chemoattractant signals as intracellular secondary signals. These signals mediate cytoskeleton rearrangement through multiple pathways, including phosphatidylinositol 3-kinase (PI3K), TORC2 complex, phospholipase A2, and phospholipase C. The activation of these signaling transduction cascades results in the local polymerization of F-actin and membrane protrusion at the leading edge of cells, which mediates directional cell migration up a gradient of chemoattractants (Artemenko et al., 2014; Kolsch et al., 2008). The molecular mechanisms responsible for EF-directed cell migration are not yet fully understood. However, it is generally believed that the major signaling networks involved in cytoskeleton rearrangements during chemotaxis, such as the PI3K/PIP3 and TORC2/PKB pathways, are also commonly used in the process of electrotaxis (Gao et al., 2015a; Tai et al., 2018; Zhao, 2009a).

Voltage-gated ion channels are crucial for a range of physiological processes. They generate and propagate electrical signals in excitable cells and muscle tissues, release neurotransmitters in pre-synaptic nerve endings, and maintain cell homeostasis (Hille, 1978). Both fruit flies and mammals possess voltage-activated K⁺ channels, such as KV1 (shaker), KV2 (shab), KV3 (shaw), KV4 (shal), KV7 (KCNQ), KV10 (Eag), KV11 (erg), KV12 (Elk), and Kca (Slo1). These channels are responsible for generating membrane potentials that drive directional movement during cell migration.

Shakers play a key role in neuronal excitability, action potential duration and frequency, and neurotransmitter release from axon terminals (Hille, 1978). Functional Shaker is composed of an assembly of four pore-forming α -subunits and four associated ancillary β -subunits, along with regulatory and scaffolding proteins (Pongs and Schwarz, 2010). The diversity of Shaker channels arises not only from the expression of different α -subunits of the KCNA protein, but also from the formation of heterotetrameric channels within this family (Jan and Jan, 2012). This assembly of different α -subunits to functional Shaker leads to distinct functional properties and targeting to neuronal compartments (Manganas and Trimmer, 2000). In the somatodendritic compartment, Shaker channels are primarily composed of Kv1.2/Kv1.6 α -subunits and regulate the creation of action potentials. Meanwhile, heteromeric Kv1.1/Kv1.2 channels are involved in the amalgamation of synaptic inputs within the axonal initial segment of hippocampal pyramidal cells. Subsequently, the controlled discharge of neurotransmitters into the synaptic cleft is subject to modulation by Kv1.1/Kv1.2 and Kv1.1/Kv1.4 channels which are present in the pre-terminal segment of axons (Ovsepián et al., 2016). The expression of native Shaker tetramers in mammalian brain has widely been investigated using channel-specific toxins (Koschak et al., 1997), or specific anti-Kv1 α -subunit antibodies (Wang et al., 1994). This paper investigates the role of Shaker in directional migration in *Dictyostelium*.

Dictyostelium discoideum is a unicellular eukaryotic microorganism use as a model system to address many important cellular processes including cell migration, cell division, phagocytosis, and development(Lee and Jeon, 2012b; Siu et al., 2011). Upon starvation, *Dictyostelium* initiates a multicellular developmental process by forming aggregates, slugs, and finally, fruiting bodies. the initial stages of this developmental process, *Dictyostelium* cells emit the chemoattractant, cAMP, which cause cells to migrate in the direction of increasing concentrations along the gradient to form aggregates(Chisholm and Firtel, 2004b).

Cells migrate directionally in response to many extracellular cues including chemical gradients (chemotaxis), topography, mechanical forces (mechanotaxis/durataxis), and electrical fields (EFs) (electrotaxis/galvanotaxis)(Barreiro et al., 2010; Berzat and Hall, 2010; Goetz, 2009).

Electric fields have long been suggested to be a candidate directional signal for cell migration in development, wound healing, and regeneration. The mechanisms used by cells to sense the weak direct current (DC) EFs, however, have remained very poorly understood.

One of the immediate effects felt by a cell upon exposure to an EF is a change in the cell membrane potentials (V_m). In an EF, the plasma membrane facing the cathode depolarizes while the membrane facing the anode hyperpolarizes (Mycielska and Djamgoz, 2004; Robinson, 1985). Trans membrane potential or ionic current changes may play a role in signal transduction and differentiation in the cellular slime mold *Dictyostelium* (van Duijn and Vogelzang, 1989). I want to find out if SLPC polarizes cells by sensing the direction of movement. In this report, *Dictyostelium* cells were used to confirm the phenotype with *slpc* null cells. This will provide a basis for indirect studies of the role of membrane potential in the regulation of intracellular K^+ .

II. MATERIALS AND METHODS

II-1. Strains and plasmid

Dictyostelium discoideum cells were obtained from the dictyostelium Stock Center, wild-type Ax2(DBS0350762, Gerry Weeks lab strain). All cells were cultured axenically in HL5 medium at 22 °C. The Knockout strains and transformants were maintained in 10 µg/ml G418.

I cloned a pair of annealed oligonucleotides into the pTM1285 vector pre-digested with *Bpi*I. For generating multiplex sgRNA vectors, I assembled sgRNA expression cassettes using the Golden Gate cloning method. Electroporation was performed using a Micro Pulser (Bio-Rad) at 0.85 kV twice with a 5 s interval. Moreover, to obtain cells transiently expressing Cas9 and sgRNA, I replaced the medium with HL5 containing 10 µg/ml of G418 after 8–16 h, and cultured the cells for another 3 days. I plated the cells on SM agar plates with *K. planticola* and incubated them for 3–4 days until plaque formation. The cloned cells obtained from SM agar plates were cultured in 24 well cells, collected, and gDNA was extracted. Using the gDNA as a template, the CRISPR target region was amplified and sequenced.

II-2. Electrotaxis assay

Dictyostelium cells were starved in DB buffer for 3 h and dropped into an electroaxis chamber as described previously (Zhao et al., 1996). Before EF stimulation, two agar salt bridges were prepared of no less than 15 cm long. The two agar salt bridges were used to connect AgCl₂ electrodes in beakers with Steinberg's solution to pools of buffer at either sides of chamber. For electric field application, the electric field strength of 15V/cm was used. The field strength was measured at the beginning and the end of the experiment (Shanley et al., 2006). For experiments with aggregation-competent cells, exponentially growing cells were washed twice and resuspended at a density of 5×10^6 cells/mL in DB buffer. The cells were pulsed with 30 nM cAMP every 6 min for 6 h. All procedures were carried out at room temperature (~22 °C). The prepared cells were seeded in an electrotactic chamber for 20 min and the unattached cells were

washed off using DB buffer. Cell migration was recorded at intervals of 1 min for 1 h using an inverted microscope (IX71; Olympus) with a camera (DS-Fi1; Nikon) controlled by the NIS-Elements software (Nikon).

II-3. Chemotaxis assay

Chemotaxis toward cAMP was performed as described previously to prepare aggregation-competent cells for the study, vegetative cells were washed twice with Na/K phosphate buffer, then resuspended in the same buffer at a density of 5×10^6 cells/ml, and pulsed with 30 nM cAMP at 6-min intervals for 5 h. Cell migration was analyzed using a Dunn Chemotaxis Chamber (SVDCC100, UK).

II-4. Quantitative analysis of cell migration

Time-lapse recordings of cell migration were analyzed using ImageJ (National Institutes of Health) as previously described. Directedness quantifies how directionally cells migrate in response to an EF. The directedness of the movement of the cells was measured as cosine θ , where θ is the angle between the direction of the field and a straight line connecting the start and end positions of the cell. Trajectory speed was assessed by dividing the total distance travelled by the cell by time. All data were obtained and analyzed from at least three independent experiments. The kinetics of directedness and trajectory speed were calculated by measuring the directedness and trajectory speed of cell migration every 2 min in a time-lapse recording and sequentially plotting the readings against time.

The images of chemotaxing cells were taken at time-lapse intervals of 6 sec for 30 min. The data were analyzed using the NIS-Elements software (Nikon) and Image J software (National Institutes of Health).

II-5. RT-PCR analysis

Total RNA from wild-type cell and *slpc* null cells was extracted by using the SV Total RNA Isolation system (Promega, Madison, WI, USA), and the cDNAs were synthesized by reverse transcription with MMLV reverse transcriptase (Promega) using random Hexamers and 5 µg of total RNAs. A Total of 5 µl cDNA was used in PCR for 35 cycles employing gene-specific primers. Universal 18S ribosomal RNA specific primers were used as an internal control.

II-5. Cell Morphology and development

The cell Morphology assay was performed as described previously. Development analyses were performed as described previously. Exponentially growing cells were harvested, washed, and then plated on Na/K phosphate agar plates at a density of 4×10^6 cells. Development was performed as described previously (Jeon et al. 2009). Exponentially growing cells were harvested and washed twice with 12 mM Na/K phosphate buffer (pH 6.1) and resuspended at a density of 3.5×10^7 cells/ml. 50 µl of the cells were placed on Na/K phosphate agar plates and developed for 24 h.

III. RESULTS

III-1. Identification of the gene encoding of SLPC

To study the function of shakers, such as potassium channels, in *Dictyostelium*, I examined the shaker-like protein domains. To identify proteins similar to SLPC, I conducted a BLASTP search via NCBI. I excluded hypothetical proteins and identified a potassium voltage gate with the closest E-value. The proteins with the closest E-values from each of the four organisms were collected and analysed for direct comparison. In *Dictyostelium*, SLPC consists of 376 amino acids. It also contains a BTB domain at the N-terminus. SLPC from *Dictyostelium* (DDB_G0277011), KV1.4 from *Homo sapiens* (AAA60034.1), Kcna4 from *Mus musculus* (AAB6068.1), egl-36 from *Caenorhabditis elegans* (NP-509795.1), and Shaker from *fruit fly* (XP_017851535.1) were used to search for SMART domains. The SLPC (DDB_G0277011) in *Dictyostelium* is similar to the Shaker channel and contains a BTB domain. It is composed of 367 amino acids (Fig. 1B). I searched the NCBI for similar BTB domains using a BLAST search, and searched for domain locations and functions in model organisms, including humans and fruit flies. I searched for domains from *Homo sapiens*, *Mus musculus*, *Caenorhabditis elegans*, and *fruit flies*, all of which showed more than 40% similarity, with a particularly high homology of 45.79% with the BTB domain of the voltage-gated potassium channel protein from *Homo sapiens*. Multiple alignment of the BTB domain allowed us to confirm the similarity of the domains and find a voltage-gated potassium channel-specific motif. This specific motif has the amino acid sequence "EYFFDR" (Fig. 1D). Conserved sequences within voltage-gated potassium channels are marked with an asterisk (*). This suggests that SLPCs in *Dictyostelium* are similar to voltage-gated potassium channels in other modal organisms and are fully functional.

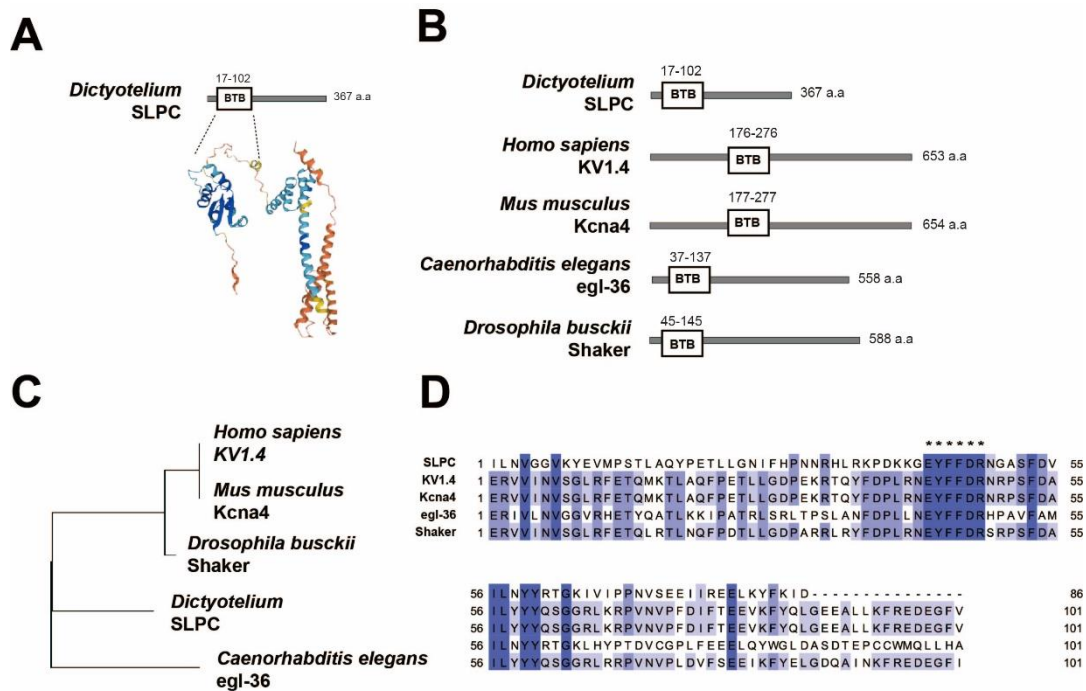


Fig. 1. Shaker-like potassium Channel domain structure and phylogenetic analysis

(A) Domain structure of the *Dictyostelium* slpc protein. Domain structure of a potassium voltage-gated channel. (B) Domain structure of BTB domain. (C) Phylogenetic tree of potassium voltage-gated channels. BTB domain sequence amino acids of Slpc and potassium voltage-gated channels were aligned by MEGA11. *Dictyostelium_Slpc* (DDB_G0277011); *Homo sapiens_KV1.4* (AAA60034.1); *Mus musculus_Kcna4* (AAB6068.1); *Caenorhabditis elegans_egl-36* (NP-509795.1); *Drosophila busckii_shaker* (XP_017851535.1). (D) Multiple alignment of the voltage-gated channel (BTB domain). The BTB domain amino acid sequence of Slpc was compared to the sequences of other potassium voltage-gated channels.

III-2. *Slpc* gene editing with CRISPR/Cas9

To investigate the role of shaker proteins in *Dictyostelium*, I generated cells in which SLPC was knocked out in *Dictyostelium*. To knockout using the CRISPR/Cas9 system, a plasmid targeting *Slpc* was generated using the pTM1285 plasmid and transfected into the cells. Twelve clones were obtained, of which cells with 215 bp inserted (#B) were used in the experiment as *slpc* null cells (Fig. 2). The gene inserted into these cells was found to be derived from a fragment of pTM1285. To confirm that the knockout was due to a genomic insertion, I performed PCR analysis of coding DNA and genomic DNA. *slpc* null cells were identified by PCR with three sets of primers and genomes. Using genomic DNA as a template, I used I/VI to confirm that Ax2 is inserted at 532 bp and *slpc* null cells at 747 bp. The two primer sets IV/VI and I/V result in no PCR product in Ax2 and a PCR product in *slpc* null cells. When the coding DNA was synthesized with I/VII primers, I obtained PCR products of 441 bp for Ax2 and 656 bp for *slpc* null cells. The IV/VI primer sets do not produce PCR products in Ax2, but do in *slpc* null cells. This PCR result shows that cell #3 is a definite *slpc* null cell (Fig. 3).

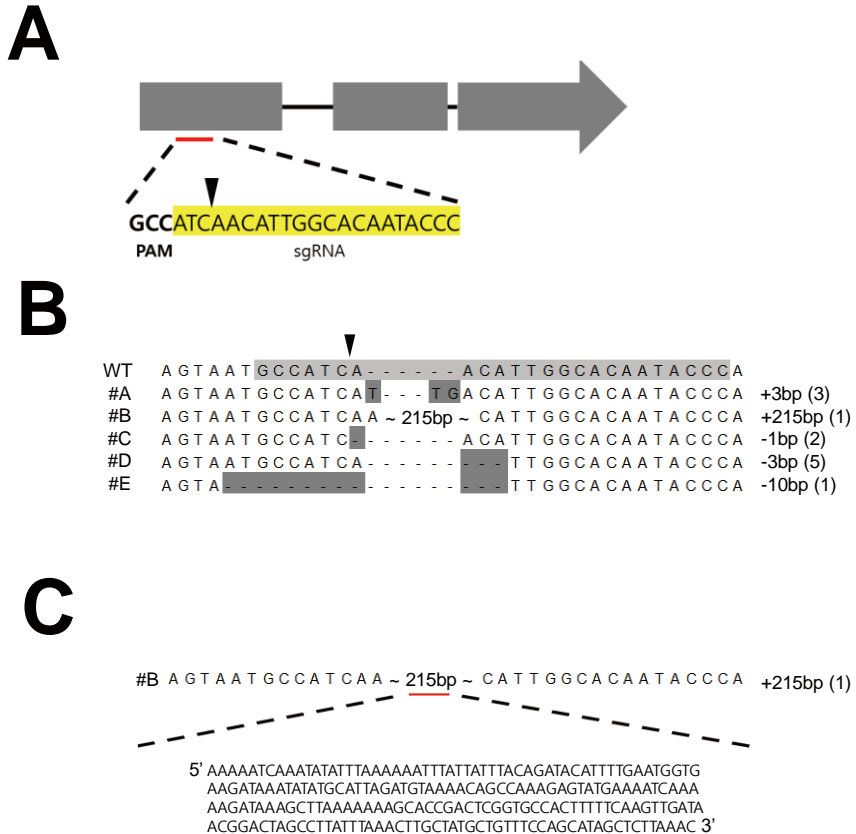


Fig. 2. Targeting of *slpC* gene using CRISPR

(A) Schematic view of sgRNA targeting locus of the *slpC* genes. The colored sequences indicate the target sites of the sgRNA (B) Wild-type sequence for *slpC* sequences derived from 5 independent positive clones by mutation detective PCR are presented. The target sequence is shown in gray colored, and mutations are shown in dark gray. Numbers in parentheses indicate the number of modified nucleotides. (C) Inserted sequence of #B.

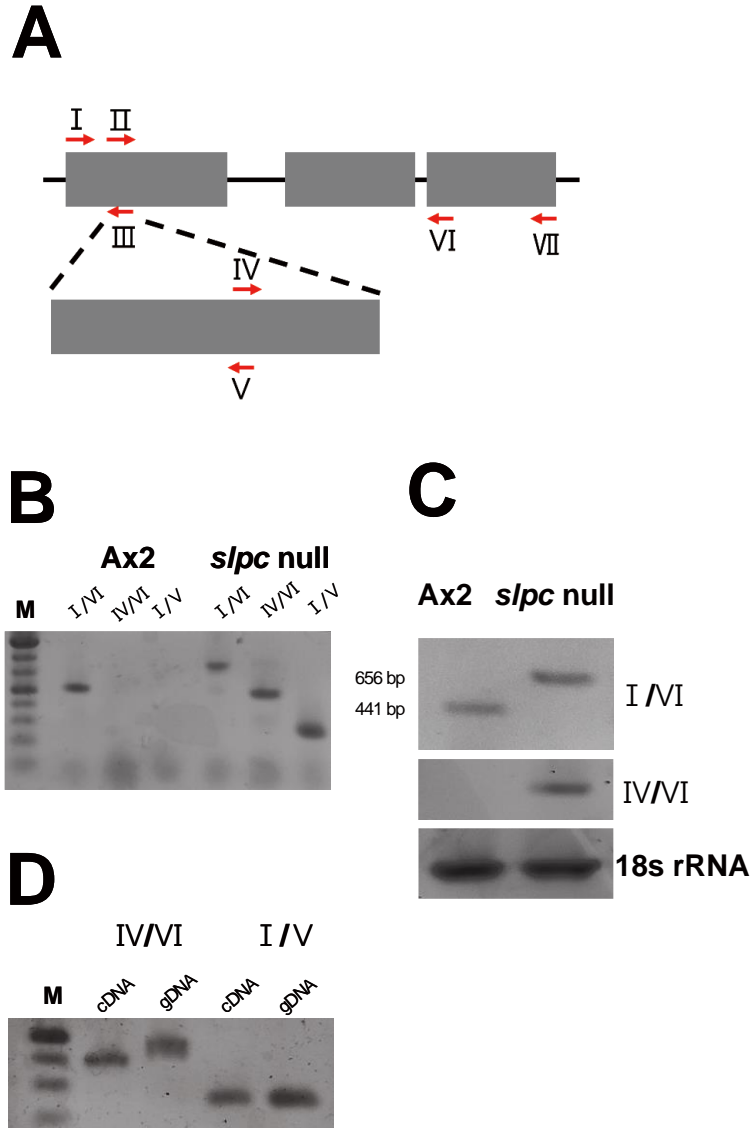


Fig. 3. Confirmation of *slpc* knockout cells

(A) Schematic diagram of *slpc* knockout constructs. Display primer sets on genomic DNA. (B) Confirmation of *slpc* gene replacement in *slpc* null cell. Genomic DNAs from wild-type cells and *slpc* null cells were extracted and used in PCR with primer set shown in panel A. (C) RT-PCR using total RNAs from wild-type and *slpc* null cells and a primer set. The universal 18S rRNA specific primers were used as an internal control. (D) Identification of gDNA and cDNA.

III-3 Morphology and development of *slpc* null cell

Dictyostelium cells live in a single-cell state under nutrient-rich conditions. Depletion of nutrients from the medium triggers the cells to aggregate, which is mediated by chemotaxis of the cells to cAMP, and the cells finally form multicellular fruiting bodies over a period of 24 h. The cells within aggregates at the initial stage of development differentiate and sort into several types of cells, form slugs, culminate, and finally form fruiting bodies consisting of dead stalks with a mass of spores on the top. To determine the roles of Slpc in multicellular developmental processes, I examined the phenotypes of *slpc* null cells during development (Fig. 4A). Wild-type cells formed aggregates at 6~10 h after starvation, slugs at 12~16 h, and then fruiting bodies within 24 h. However, cells lacking Slpc displayed severely aberrant multicellular developmental processes after initially forming normal-looking mounds. *slpc* null cells produced multiple tips on mounds and multiple developmental structures arising from a single mound, whereas wild-type cells formed a tip from one mound and fruiting bodies containing one stalk and one sorus on the top. To investigate the function of SLPC in various processes such as developmental status and cell morphogenesis, I examined functions such as morphogenetic cell motility and development. The wide type, Ax2, is morphologically rounded and has the appearance of a normal cell. *slpc* null cells have a smaller size than the wild type (Fig. 4 B C).

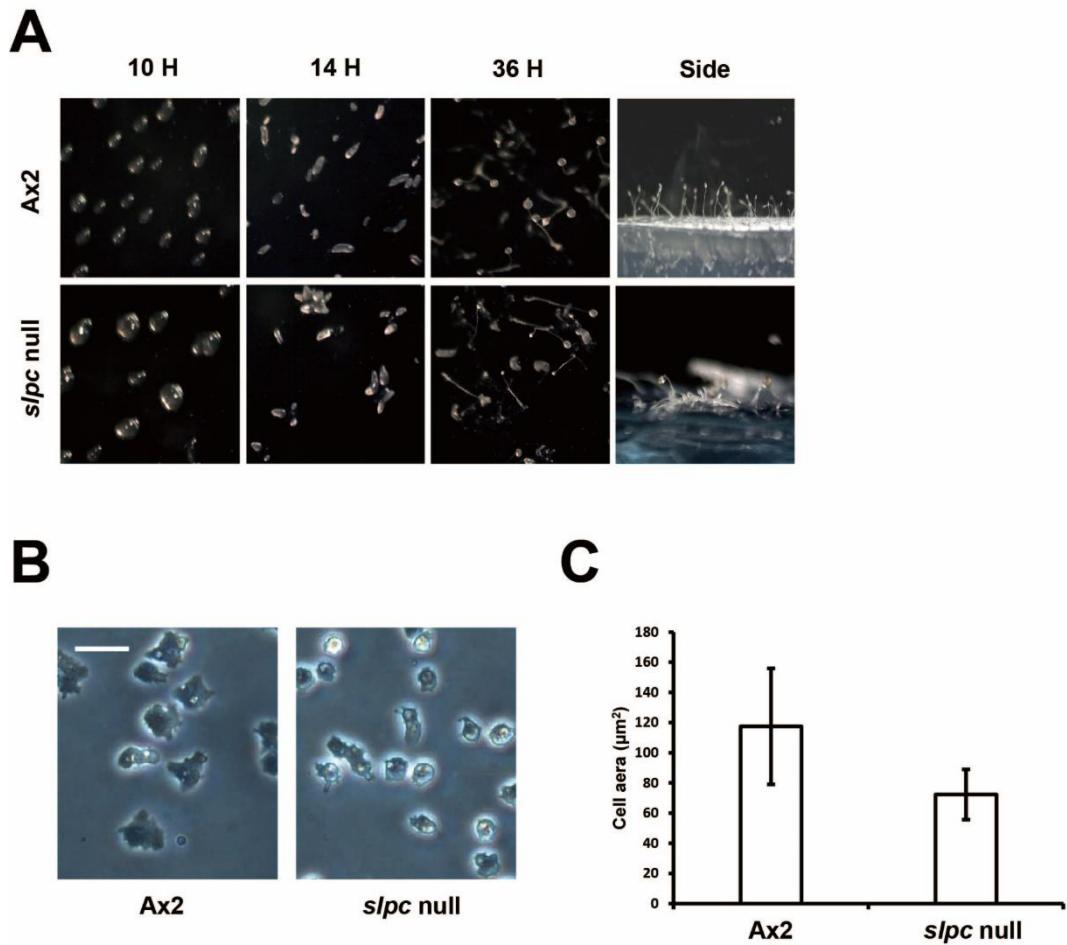


Fig. 4. Morphology and Development of the *slpc* null cells

(A) Developmental phenotypes of the cells on non-nutrient agar plates. Exponentially growing cells were washed and plated on non-nutrient agar plates. Photographs were taken at the indicated times after plating and representative developmental images at the developmental stages were shown. (B) Morphology of the cells. Wild-type and *slpc* null cells were photographed. Scale bar, 20 µm. (C) Analysis of the cell area. The mean values were graphed. Data are represented as mean ± S.D. from three independent experiments.

III-4 Electrotaxis of *slpc* null cell

The effects of extracellular pH and K^+ on electricity accumulation were reported using *Dictyostelium* cells, which have the unique property of being able to tolerate changes in extracellular pH, K^+ , and even electroporation while maintaining good motility. They found that changes in extracellular pH, K^+ , and electroporation significantly affected V_m , and that reducing V_m in response to these three factors significantly inhibited electricity accumulation. The inhibitory effect on electromigration correlated well with reduced V_m , but the chemical effect did not. For a deeper understanding of the role of K^+ in electrotaxis, I investigated the role of electrotaxis in *slpc* null cells.

Cell migration was monitored for 60 min. No EF was applied for the first 10 min, 15 V/cm EF was applied for the following 30 min, and cell migration was recorded without EF stimulation for the final 20 min. To understand the role of *Slpc* in EF-induced cell migration, Upon EF stimulation, wild-type cells showed directional migration towards the cathode. I examined directional and trajectory speeds upon EF exposure in *slpc* null cells and compared them to wild-type Ax2 cells. *slpc* null cells showed increased migration velocity in EF. *slpc* null cells showed half the speed of wild-type. At EF, Ax2 showed a speed of 5.4 $\mu\text{m}/\text{min}$, while *slpc* null cells showed a speed of 2.9 $\mu\text{m}/\text{min}$. (Fig. 5B).

Since different cell states express different genes, I performed the same experiment using cells in the aggregation-competent state. Consistent with previous experiments, the *slpc* null cells are significantly less mobile than their wild-type counterparts, the Ax2 cells (Fig. 6). This suggests that *Slpc* acts to increase the basic speed of cell movement

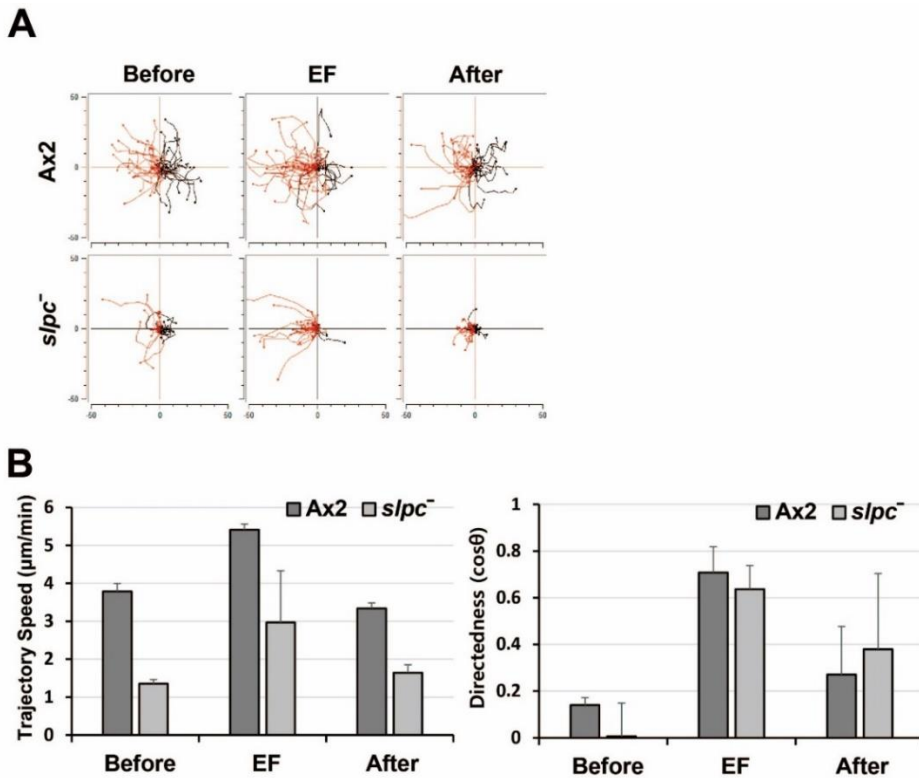


Fig. 5. Electrotaxis of wild-type cells and *slpc* null cells on the vegetative conditions

(A) Trajectories of wild-type Ax2 cells and *slpc* null cell in an electric field (EF) of 15 V/cm. EF-directed cell migration was recorded at time-lapse intervals of 1 min for 60 min. EF of 15 V/cm was applied from the 10 to 40 min mark during recording. No EF was applied for the first 10 min and the last 20 min. “Before” indicates the period of time during the first 10 min without EF application. “EF” indicates the 10-min period after commencement of EF stimulation (20 to 30 min). “After” indicates the 10 min period after EF stimulation was stopped. Plots show migration paths of the cells with the start position of each cell centered at point 0,0. An arrow indicates the direction of the EFs. (B) Quantitative analyses of the directional migration of wild-type cells and *slpc* null cell in an EF. Quantitative values of directedness and trajectory speed of *slpc* null cells in an EF of 15V/cm were compared with those of wild-type Ax2. Data are represented as mean ± S.D. from three independent experiments.

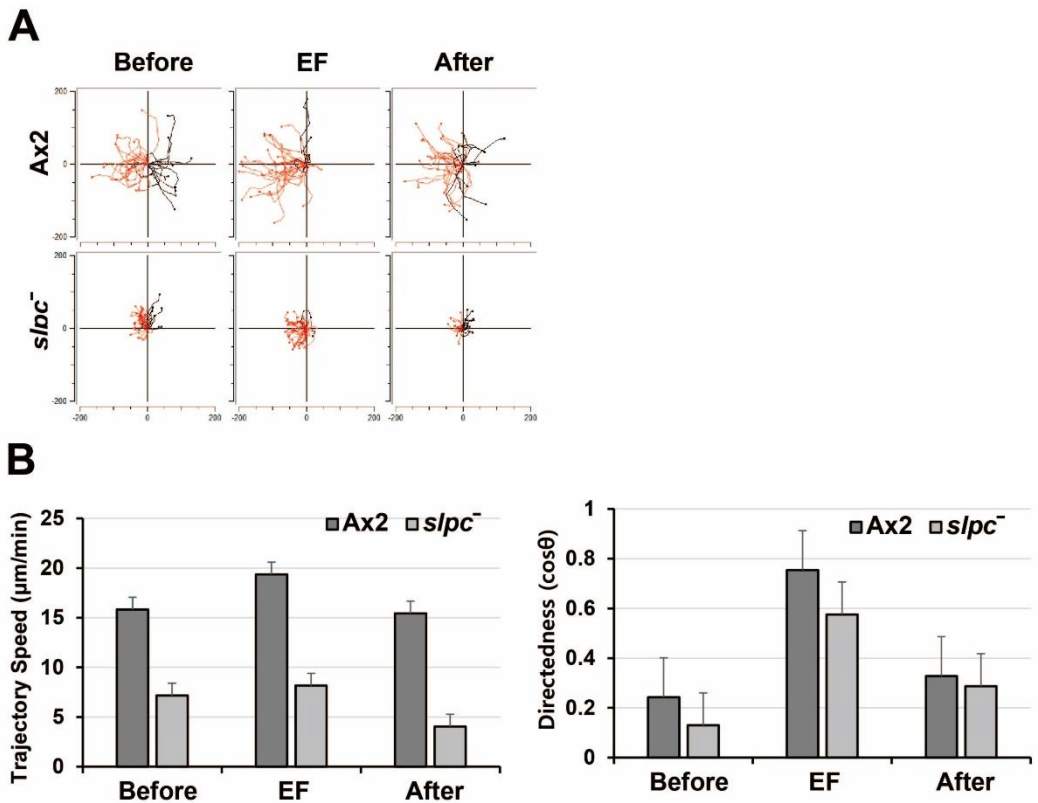


Fig. 6. Electrotaxis of wild-type cells and *slpc* null cells on the aggregation-competent conditions

(A) Trajectories of *slpc* null cells and wild-type cells at an EF of 15 V/cm in aggregation-competent conditions. (B) Quantitative analysis of directional migration of *slpc* null cells. Data are represented as mean \pm S.D. from three independent experiments.

III-5 Chemotaxis of *slpc* null cell

Since *slpc* null cells showed lower motility compared to wild-type during electrotaxis, I experimented to determine what phenotype they exhibit during chemotaxis. I performed the chemotaxis assay with wild-type, *slpc* null cells using a Dunn chemotaxis chamber (Fig. 7A). To prepare aggregation-competent cells for study, vegetative cells were washed twice with Na/K phosphate buffer, then resuspended in the same buffer at a density of 5×10^6 cells/ml and pulsed with 30 nM cAMP every 6 min for 5 h. Wild-type cells moved at 20.2 $\mu\text{m}/\text{min}$ toward the cAMP source. In contrast, *slpc* null cells had significantly low moving speed with 13.8 $\mu\text{m}/\text{min}$ (Fig. 7B). In directionality, which is the index showing how straight the cells move, all of the cells including wild-type and *slpc* null cells showed no significant difference (Fig. 7B). These results suggest that SLPC is involved in the regulation of the speed but not the direction of migration during chemotaxis. These results suggest that SLPC proteins are required to regulate cell migration rates during chemotaxis cell migration.

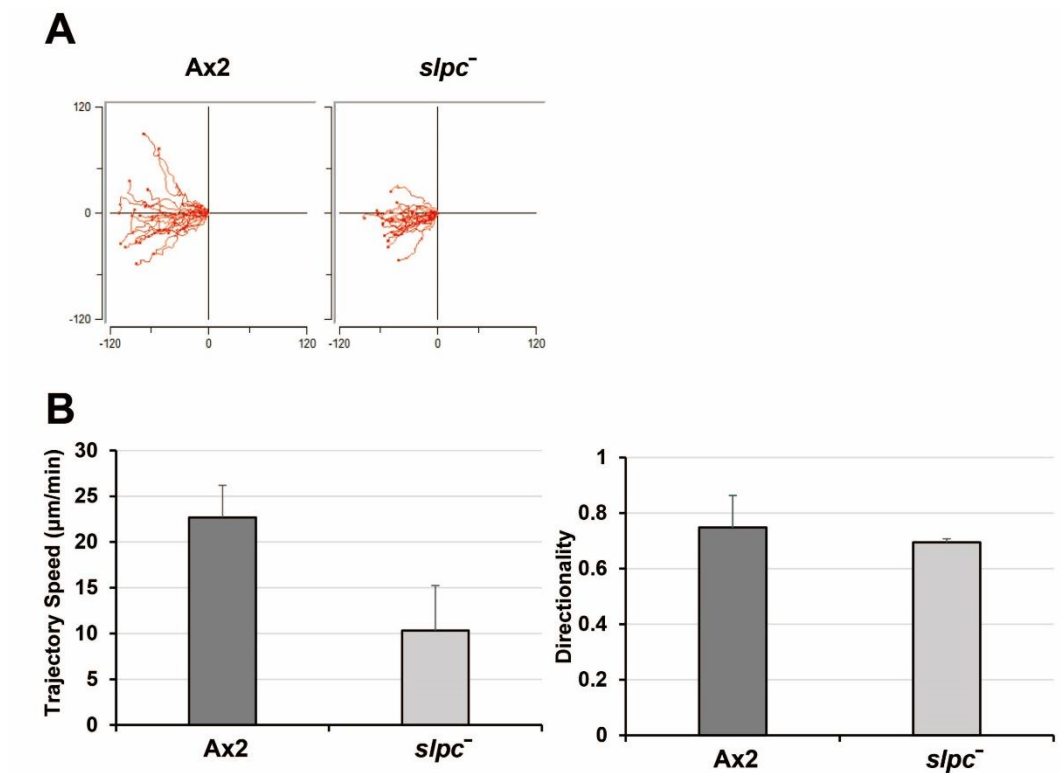


Fig. 7. Chemotaxis of wild-type cells and *slpc* null cells on the aggregation-competent conditions

Aggregation competent wild-type cells or *slpc* null cells were placed in a Dunn chemotaxis chamber, and the motility of cells towards cAMP gradient were analyzed. The cell migration was recorded at time lapse intervals of 6 sec for 30 min. (A) Trajectories of migrating cells in the Dunn chemotaxis chamber towards cAMP. Each line indicates the track of single cell chemotaxing towards cAMP. (B) Quantification of the cell motility of chemotaxing cells. The recorded images were analyzed by NIS-element software. Directionality measures how straightly cells move. The direction of cell moving in a straight line is 1. Trajectory speed is the total distance traveled by the cell divided by the time. Data are represented as mean \pm S.D. from three independent experiments.

IV. DISCUSSION

I used the CRISPR/Cas9 system to create *slpc* null cells and examined them in development, morphology, and electrotaxis to understand the role of Shaker protein. Embryologically, while the wild-type exhibited normal development, the *slpc* null cells formed mounds larger in size than the wild-type, and subsequently exhibited a multi-stranded slug morphology, unlike the wild-type, where the slug extends in a single strand. These defects in development suggest that Slpc plays an important role in shaping organization during development. In mice, the KV1.1 Channel, known as the Shaker protein subfamily, has been reported to regulate early postnatal neurogenesis through the TrkB signaling pathway (Chou et al., 2021). These findings suggest that intracellular ion regulation is important for *Dictyostelium* development. To investigate the role of cell migration in electrical stimulation of Slpc, I performed electrotaxis experiments. Compared to the Wild-type, *slpc* null cells were about half as slow, with no significant difference in directionality. The reduced migration rate of *slpc* null cells appears to be caused by dysregulation of intracellular K^+ . For *Dictyostelium* cells to electrotaxis, the formation of a proper membrane potential is required. Previously, it was reported that the speed and direction of electrotaxis was inhibited by manipulation of external potassium concentration (Gao et al., 2011). To investigate this further, it is necessary to examine whether cells lacking SLPC are actually defective in their membrane potential during migration. It is also necessary to experiment with *slpc* null cells and SLPC-complemented cells to confirm this. This suggests that the regulation of membrane potential is critical for cell migration speed and that SLPC is involved. I believe that the role of SLPC deserves further clarification and in-depth study.

CONCLUSION

The study investigates the shared mechanisms underlying chemotaxis and electrotaxis, focusing on key players: PI3Ks, DydA, and Shaker-like potassium channels (SLPC). These components play critical roles in cell motility, migration, and development.

PI3Ks (Phosphatidylinositol 3-Kinases) : In chemotaxis, PI3Ks play a crucial role in relaying and amplifying chemoattractant signals, mediating rearrangements of the actin cytoskeleton. Unexpectedly, in electrotaxis, the role of PI3Ks varies based on the cell state. In vegetative *Dictyostelium* cells, PI3K inhibition increases motility, suggesting a suppressive role in regulating cell motility in vegetative cells.

The observation that cell motility increases with the progression of developmental stages in *Dictyostelium* aligns with existing literature. It has been proposed that as cells transition to the aggregation-competent stage, they secrete signaling molecules in response to external electric fields (EF), which induce cell motility and electrical sensing. These signaling molecules likely play a role in coordinating cell migration by regulating cAMP signal transduction, including the activation of Ca^{2+} influx, adenylyl cyclases, guanyl cyclases, and cGMP signaling. The study's results indicating a role for PI3K in regulating cell motility during various developmental phases in *Dictyostelium* suggest a complex interplay between PI3K-mediated lipid signaling and cAMP/cGMP signaling. However, the mechanism underlying the suppression of motility in vegetative cells due to PI3K inhibition or removal remains unknown. To gain a deeper understanding, further exploration into the relationship between PI3K-mediated lipid signaling and cAMP/cGMP signaling is proposed. This investigation could unveil how these pathways intersect and influence each other to regulate cell motility throughout different developmental stages. This could involve examining the downstream targets and interactions of PI3K within the context of cAMP and cGMP signaling pathways. Such research endeavors would contribute valuable insights into the regulatory mechanisms governing cell motility in the dynamic context of *Dictyostelium* development.

DydA (Daydreamer) : DydA acts as an adaptor protein connecting Ras signaling and cytoskeletal rearrangement in chemotaxis, development, and cell growth. Upon chemoattractant stimulation, DydA rapidly translocates to the cell cortex through its RA domain and PRM region, playing a vital role in controlling cell polarity and pseudopodia formation. The PRM region is crucial for mediating the localization of DydA to the cell cortex and actin foci in response to chemoattractant stimulation. The protein DydA in *Dictyostelium discoideum* plays a crucial role in actin cytoskeleton reorganization, influencing cell polarization, morphology, and migration. Cells lacking DydA exhibit significant reductions in polarization, migration speed, and directionality toward a cAMP source. *DydA* null cells display numerous micro-spikes and elevated levels of F-actin compared to wild-type cells, suggesting that DydA may play an inhibitory role in F-actin assembly. The study indicates that DydA is involved in recruiting to the site of F-actin assembly, particularly in the anterior region of migrating cells and actin foci at the bottom. This recruitment is mediated by the RA1 domain and the PRM (proline-rich motif) region of DydA. The PRM region likely plays a crucial role in mediating protein-protein interactions, as proline-rich sequences are known to be involved in various protein-protein interactions. The polyproline type II (PPII) helix, formed by proline residues, is implicated in these interactions. Proline-rich sequences are recognized by various protein domains, including the SH3 domain, WW domain, EVH1 domain, and profilin. DydA's PRM region may similarly participate in interactions with other proteins involved in actin cytoskeletal rearrangements. Identifying the binding partner of DydA through the PRM region could provide valuable insights into the signaling mechanisms from Ras signaling to downstream effectors such as PI3Ks, Akt/Pkb, and, ultimately, the actin cytoskeleton. This intricate interplay between DydA, RasG, and the actin cytoskeleton underscores the complexity of cellular processes and the importance of understanding these molecular mechanisms for comprehending cell migration, morphology, and overall cellular behavior.

Shaker-like Potassium Channels (SLPC) : SLPC, a Shaker family protein and a voltage-gated potassium channel, is involved in neurotransmitter release, heart rate, and muscle

contraction. In *Dictyostelium*, SLPC knockout results in smaller cells, altered electric field-directed migration with slightly reduced speed, and aberrant multicellular structures in development. These findings suggest roles for SLPC in electrotaxis and development. Overall, this study contributes to understanding the intricate biological processes specific to electrotaxis and chemotaxis.

Overall, the role of PI3K depends on the cell state: in the vegetative state, PI3K acts as a rate suppressor. DydA localizes for cell migration through RA1 and PRM. SLPC regulates the rate of cell development and migration. The characterization of these three proteins provides new insights into the molecular mechanisms underlying directional cell migration.

REFERENCES

- Armitage, J.P., and Hellingwerf, K.J. (2003). Light-induced behavioral responses (phototaxis) in prokaryotes. *Photosynth Res* 76, 145-155. 10.1023/a:1024974111818.
- Artemenko, Y., Lampert, T.J., and Devreotes, P.N. (2014). Moving towards a paradigm: common mechanisms of chemotactic signaling in Dictyostelium and mammalian leukocytes. *Cell Mol Life Sci* 71, 3711-3747. 10.1007/s00018-014-1638-8.
- Bagorda, A., and Parent, C.A. (2008). Eukaryotic chemotaxis at a glance. *J Cell Sci* 121, 2621-2624. 10.1242/jcs.018077.
- Barreiro, O., Martin, P., Gonzalez-Amaro, R., and Sanchez-Madrid, F. (2010). Molecular cues guiding inflammatory responses. *Cardiovasc Res* 86, 174-182. 10.1093/cvr/cvq001.
- Baumgardner, K., Lin, C., Firtel, R.A., and Lacal, J. (2018). Phosphodiesterase PdeD, dynacortin, and a Kelch repeat-containing protein are direct GSK3 substrates in Dictyostelium that contribute to chemotaxis towards cAMP. *Environ Microbiol* 20, 1888-1903. 10.1111/1462-2920.14126.
- Berzat, A., and Hall, A. (2010). Cellular responses to extracellular guidance cues. *EMBO J* 29, 2734-2745. 10.1038/emboj.2010.170.
- Bosgraaf, L., Keizer-Gunnink, I., and Van Haastert, P.J. (2008). PI3-kinase signaling contributes to orientation in shallow gradients and enhances speed in steep chemoattractant gradients. *J Cell Sci* 121, 3589-3597. 10.1242/jcs.031781.
- Bosgraaf, L., and van Haastert, P.J. (2006). The regulation of myosin II in Dictyostelium. *Eur J Cell Biol* 85, 969-979. 10.1016/j.ejcb.2006.04.004.
- Chisholm, R.L., and Firtel, R.A. (2004a). Insights into morphogenesis from a simple developmental system. *Nature reviews Molecular cell biology* 5, 531-541.
- Chou, S.M., Li, K.X., Huang, M.Y., Chen, C., Lin King, Y.H., Li, G.G., Zhou, W., Teo, C.F., Jan, Y.N., Jan, L.Y., and Yang, S.B. (2021). Kv1.1 channels regulate early postnatal neurogenesis in mouse hippocampus via the TrkB signaling pathway. *Elife* 10. 10.7554/eLife.58779.
- Clarke, M., and Gomer, R. (1995). PSF and CMF, autocrine factors that regulate gene expression during growth and early development of Dictyostelium. *Experientia* 51, 1124-1134.

- De Lozanne, A., and Spudich, J.A. (1987). Disruption of the Dictyostelium myosin heavy chain gene by homologous recombination. *Science* 236, 1086-1091. 10.1126/science.3576222.
- Firat-Karalar, E.N., and Welch, M.D. (2011). New mechanisms and functions of actin nucleation. *Curr Opin Cell Biol* 23, 4-13. 10.1016/j.ceb.2010.10.007.
- Funamoto, S., Meili, R., Lee, S., Parry, L., and Firtel, R.A. (2002). Spatial and temporal regulation of 3-phosphoinositides by PI 3-kinase and PTEN mediates chemotaxis. *Cell* 109, 611-623. 10.1016/s0092-8674(02)00755-9.
- Funamoto, S., Milan, K., Meili, R., and Firtel, R.A. (2001). Role of phosphatidylinositol 3' kinase and a downstream pleckstrin homology domain-containing protein in controlling chemotaxis in dictyostelium. *J Cell Biol* 153, 795-810. 10.1083/jcb.153.4.795.
- Gao, R., Zhao, S., Jiang, X., Sun, Y., Zhao, S., Gao, J., Borleis, J., Willard, S., Tang, M., Cai, H., et al. (2015a). A large-scale screen reveals genes that mediate electrotaxis in Dictyostelium discoideum. *Sci Signal* 8, ra50. 10.1126/scisignal.aab0562.
- Gao, R.C., Zhang, X.D., Sun, Y.H., Kamimura, Y., Mogilner, A., Devreotes, P.N., and Zhao, M. (2011). Different roles of membrane potentials in electrotaxis and chemotaxis of dictyostelium cells. *Eukaryot Cell* 10, 1251-1256. 10.1128/EC.05066-11.
- Gao, R.C., Zhao, S.W., Jiang, X.P., Sun, Y.H., Zhao, S.J., Gao, J., Borleis, J., Willard, S., Tang, M., Cai, H.Q., et al. (2015b). A large-scale screen reveals genes that mediate electrotaxis in. *Science Signaling* 8, ra50-ra50. ARTN ra50 10.1126/scisignal.aab0562.
- Goetz, J.G. (2009). Bidirectional control of the inner dynamics of focal adhesions promotes cell migration. *Cell Adh Migr* 3, 185-190. 10.4161/cam.3.2.7295.
- Guido, I., Diehl, D., Olszok, N.A., and Bodenschatz, E. (2020). Cellular velocity, electrical persistence and sensing in developed and vegetative cells during electrotaxis. *PLoS One* 15, e0239379. 10.1371/journal.pone.0239379.
- Hille, B. (1978). Ionic channels in excitable membranes. Current problems and biophysical approaches. *Biophys J* 22, 283-294. 10.1016/S0006-3495(78)85489-7.

- Hoeller, O., and Kay, R.R. (2007). Chemotaxis in the absence of PIP3 gradients. *Curr Biol* *17*, 813-817. 10.1016/j.cub.2007.04.004.
- Humphries, C.L., Balcer, H.I., D'Agostino, J.L., Winsor, B., Drubin, D.G., Barnes, G., Andrews, B.J., and Goode, B.L. (2002). Direct regulation of Arp2/3 complex activity and function by the actin binding protein coronin. *J Cell Biol* *159*, 993-1004. 10.1083/jcb.200206113.
- Jan, L.Y., and Jan, Y.N. (2012). Voltage-gated potassium channels and the diversity of electrical signalling. *J Physiol* *590*, 2591-2599. 10.1113/jphysiol.2011.224212.
- Jeon, T.J., Gao, R., Kim, H., Lee, A., Jeon, P., Devreotes, P.N., and Zhao, M. (2019). Cell migration directionality and speed are independently regulated by RasG and Gbeta in Dictyostelium cells in electrotaxis. *Biol Open* *8*, bio042457. 10.1242/bio.042457.
- Jeon, T.J., Lee, D.J., Merlot, S., Weeks, G., and Firtel, R.A. (2007). Rap1 controls cell adhesion and cell motility through the regulation of myosin II. *Journal of Cell Biology* *176*, 1021-1033. DOI 10.1083/jcb.200607072.
- Jeon, T.J.e.a. (2007). Regulation of Rap1 activity by RapGAP1 controls cell adhesion at the front of chemotaxing cells. *Journal of Cell Biology* *179*, 833-843. 10.1083/jcb.200705068.
- Jin, T., Xu, X., Fang, J., Isik, N., Yan, J., Brzostowski, J.A., and Hereld, D. (2009). How human leukocytes track down and destroy pathogens: lessons learned from the model organism Dictyostelium discoideum. *Immunol Res* *43*, 118-127. 10.1007/s12026-008-8056-7.
- Khezri, M.R., Jafari, R., Yousefi, K., and Zolbanin, N.M. (2022). The PI3K/AKT signaling pathway in cancer: Molecular mechanisms and possible therapeutic interventions. *Exp Mol Pathol* *127*, 104787. 10.1016/j.yexmp.2022.104787.
- Kim, H., Shin, D.Y., and Jeon, T.J. (2017). Minimal amino acids in the I/LWEQ domain required for anterior/posterior localization in Dictyostelium. *J Microbiol* *55*, 366-372. 10.1007/s12275-017-6550-0.
- Koch, P.A., Dornan, G.L., Hessenberger, M., and Haucke, V. (2021). The molecular mechanisms mediating class II PI 3-kinase function in cell physiology. *FEBS J* *288*, 7025-7042. 10.1111/febs.15692.

- Kolsch, V., Charest, P.G., and Firtel, R.A. (2008). The regulation of cell motility and chemotaxis by phospholipid signaling. *J Cell Sci* 121, 551-559. 10.1242/jcs.023333.
- Kölsch, V., Shen, Z., Lee, S., Plak, K., Lotfi, P., Chang, J., Charest, P.G., Romero, J.L., Jeon, T.J., and Kortholt, A. (2013). Daydreamer, a Ras effector and GSK-3 substrate, is important for directional sensing and cell motility. *Molecular biology of the cell* 24, 100-114.
- Kolsch, V., Shen, Z., Lee, S., Plak, K., Lotfi, P., Chang, J., Charest, P.G., Romero, J.L., Jeon, T.J., Kortholt, A., et al. (2013). Daydreamer, a Ras effector and GSK-3 substrate, is important for directional sensing and cell motility. *Mol Biol Cell* 24, 100-114. 10.1091/mbc.E12-04-0271.
- Kortholt, A., and van Haastert, P.J. (2008). Highlighting the role of Ras and Rap during Dictyostelium chemotaxis. *Cell Signal* 20, 1415-1422. 10.1016/j.cellsig.2008.02.006.
- Koschak, A., Koch, R.O., Liu, J., Kaczorowski, G.J., Reinhart, P.H., Garcia, M.L., and Knaus, H.G. (1997). [125I]Iberitoxin-D19Y/Y36F, the first selective, high specific activity radioligand for high-conductance calcium-activated potassium channels. *Biochemistry* 36, 1943-1952. 10.1021/bi962074m.
- Krause, M., Leslie, J.D., Stewart, M., Lafuente, E.M., Valderrama, F., Jagannathan, R., Strasser, G.A., Rubinson, D.A., Liu, H., and Way, M. (2004). Lamellipodin, an Ena/VASP ligand, is implicated in the regulation of lamellipodial dynamics. *Developmental cell* 7, 571-583.
- Lafuente, E.M., van Puijenbroek, A.A., Krause, M., Carman, C.V., Freeman, G.J., Berezovskaya, A., Constantine, E., Springer, T.A., Gertler, F.B., and Boussiotis, V.A. (2004). RIAM, an Ena/VASP and Profilin ligand, interacts with Rap1-GTP and mediates Rap1-induced adhesion. *Dev Cell* 7, 585-595. 10.1016/j.devcel.2004.07.021.
- Lee, C.S., Choi, C.K., Shin, E.Y., Schwartz, M.A., and Kim, E.G. (2010). Myosin II directly binds and inhibits Dbl family guanine nucleotide exchange factors: a possible link to Rho family GTPases. *J Cell Biol* 190, 663-674. 10.1083/jcb.201003057.
- Lee, M.-R., and Jeon, T.J. (2012). Cell migration: regulation of cytoskeleton by Rap1 in Dictyostelium discoideum. *Journal of Microbiology* 50, 555-561.
- Lee, M.R., Kim, H., and Jeon, T.J. (2014). The I/LWEQ domain in RapGAP3 required for posterior localization in migrating cells. *Mol Cells* 37, 307-313. 10.14348/molcells.2014.2309.

- Li, S.S. (2005). Specificity and versatility of SH3 and other proline-recognition domains: structural basis and implications for cellular signal transduction. *Biochem J* 390, 641-653. 10.1042/BJ20050411.
- Lo, C.M., Wang, H.B., Dembo, M., and Wang, Y.L. (2000). Cell movement is guided by the rigidity of the substrate. *Biophys J* 79, 144-152. 10.1016/s0006-3495(00)76279-5.
- Loovers, H.M., Postma, M., Keizer-Gunnink, I., Huang, Y.E., Devreotes, P.N., and van Haastert, P.J. (2006). Distinct roles of PI(3,4,5)P3 during chemoattractant signaling in Dictyostelium: a quantitative in vivo analysis by inhibition of PI3-kinase. *Mol Biol Cell* 17, 1503-1513. 10.1091/mbc.e05-09-0825.
- Mahoney, N.M., Rozwarski, D.A., Fedorov, E., Fedorov, A.A., and Almo, S.C. (1999). Profilin binds proline-rich ligands in two distinct amide backbone orientations. *Nat Struct Biol* 6, 666-671. 10.1038/10722.
- Manganas, L.N., and Trimmer, J.S. (2000). Subunit composition determines Kv1 potassium channel surface expression. *J Biol Chem* 275, 29685-29693. 10.1074/jbc.M005010200.
- McLaughlin, K.A., and Levin, M. (2018a). Bioelectric signaling in regeneration: mechanisms of ionic controls of growth and form. *Developmental biology* 433, 177-189.
- McLaughlin, K.A., and Levin, M. (2018b). Bioelectric signaling in regeneration: Mechanisms of ionic controls of growth and form. *Dev Biol* 433, 177-189. 10.1016/j.ydbio.2017.08.032.
- Meili, R., Alonso-Latorre, B., del Alamo, J.C., Firtel, R.A., and Lasheras, J.C. (2010). Myosin II is essential for the spatiotemporal organization of traction forces during cell motility. *Mol Biol Cell* 21, 405-417. 10.1091/mbc.e09-08-0703.
- Mycielska, M.E., and Djamgoz, M.B. (2004). Cellular mechanisms of direct-current electric field effects: galvanotaxis and metastatic disease. *J Cell Sci* 117, 1631-1639. 10.1242/jcs.01125.
- Ovsepián, S.V., LeBerre, M., Steuber, V., O'Leary, V.B., Leibold, C., and Oliver Dolly, J. (2016). Distinctive role of KV1.1 subunit in the biology and functions of low threshold K(+) channels with implications for neurological disease. *Pharmacol Ther* 159, 93-101. 10.1016/j.pharmthera.2016.01.005.

- Pongs, O., and Schwarz, J.R. (2010). Ancillary subunits associated with voltage-dependent K⁺ channels. *Physiol Rev* *90*, 755-796. 10.1152/physrev.00020.2009.
- Prehoda, K.E., Lee, D.J., and Lim, W.A. (1999). Structure of the enabled/VASP homology 1 domain-peptide complex: a key component in the spatial control of actin assembly. *Cell* *97*, 471-480. 10.1016/s0092-8674(00)80757-6.
- Raaijmakers, J.H., and Bos, J.L. (2009). Specificity in Ras and Rap signaling. *J Biol Chem* *284*, 10995-10999. 10.1074/jbc.R800061200.
- Ramot, D., MacInnis, B.L., and Goodman, M.B. (2008). Bidirectional temperature-sensing by a single thermosensory neuron in *C. elegans*. *Nat Neurosci* *11*, 908-915. 10.1038/nn.2157.
- Ravi Chandra, B., Gowthaman, R., Akhouri, R.R., Gupta, D., and Sharma, A. (2004). Distribution of proline-rich (PxxP) motifs in distinct proteomes: functional and therapeutic implications for malaria and tuberculosis. *Protein Eng Des Sel* *17*, 175-182. 10.1093/protein/gzh024.
- Ridley, A.J., Schwartz, M.A., Burridge, K., Firtel, R.A., Ginsberg, M.H., Borisy, G., Parsons, J.T., and Horwitz, A.R. (2003). Cell migration: integrating signals from front to back. *Science* *302*, 1704-1709. 10.1126/science.1092053.
- Robinson, K.R. (1985). The responses of cells to electrical fields: a review. *J Cell Biol* *101*, 2023-2027. 10.1083/jcb.101.6.2023.
- Rodal, A.A., Sokolova, O., Robins, D.B., Daugherty, K.M., Hippenmeyer, S., Riezman, H., Grigorieff, N., and Goode, B.L. (2005). Conformational changes in the Arp2/3 complex leading to actin nucleation. *Nat Struct Mol Biol* *12*, 26-31. 10.1038/nsmb870.
- Romero, J.L., Shen, Z., Baumgardner, K., Wei, J., Briggs, S.P., and Firtel, R.A. (2018). The Dictyostelium GSK3 kinase GlkA coordinates signal relay and chemotaxis in response to growth conditions. *Developmental biology* *435*, 56-72.
- Sasaki, A.T., Chun, C., Takeda, K., and Firtel, R.A. (2004). Localized Ras signaling at the leading edge regulates PI3K, cell polarity, and directional cell movement. *The Journal of cell biology* *167*, 505-518.
- Sasaki, A.T., and Firtel, R.A. (2006). Regulation of chemotaxis by the orchestrated activation of Ras, PI3K, and TOR. *Eur J Cell Biol* *85*, 873-895. 10.1016/j.ejcb.2006.04.007.

- Sato, M.J., Kuwayama, H., van Egmond, W.N., Takayama, A.L., Takagi, H., van Haastert, P.J., Yanagida, T., and Ueda, M. (2009). Switching direction in electric-signal-induced cell migration by cyclic guanosine monophosphate and phosphatidylinositol signaling. *Proc Natl Acad Sci U S A* *106*, 6667-6672. 10.1073/pnas.0809974106.
- Schweimer, K., Hoffmann, S., Bauer, F., Friedrich, U., Kardinal, C., Feller, S.M., Biesinger, B., and Sticht, H. (2002). Structural investigation of the binding of a herpesviral protein to the SH3 domain of tyrosine kinase Lck. *Biochemistry* *41*, 5120-5130. 10.1021/bi015986j.
- Shanley, L.J., Walczysko, P., Bain, M., MacEwan, D.J., and Zhao, M.J.J.C.S. (2006). Influx of extracellular Ca²⁺ is necessary for electrotaxis in *Dictyostelium*. *119*, 4741-4748.
- Siu, C.H., Sriskanthadevan, S., Wang, J., Hou, L., Chen, G., Xu, X., Thomson, A., and Yang, C. (2011). Regulation of spatiotemporal expression of cell-cell adhesion molecules during development of *Dictyostelium discoideum*. *Dev Growth Differ* *53*, 518-527. 10.1111/j.1440-169X.2011.01267.x.
- Stephens, G.J., Johnson-Kerner, B., Bialek, W., and Ryu, W.S. (2008). Dimensionality and dynamics in the behavior of *C. elegans*. *PLoS Comput Biol* *4*, e1000028. 10.1371/journal.pcbi.1000028.
- Tai, G., Tai, M., and Zhao, M. (2018). Electrically stimulated cell migration and its contribution to wound healing. *Burns Trauma* *6*, 20. 10.1186/s41038-018-0123-2.
- Uchida, K.S., and Yumura, S. (2004). Dynamics of novel feet of *Dictyostelium* cells during migration. *J Cell Sci* *117*, 1443-1455. 10.1242/jcs.01015.
- van Duijn, B., and Vogelzang, S.A. (1989). The membrane potential of the cellular slime mold *Dictyostelium discoideum* is mainly generated by an electrogenic proton pump. *Biochim Biophys Acta* *983*, 186-192. 10.1016/0005-2736(89)90232-0.
- Wang, H., Kunkel, D.D., Schwartzkroin, P.A., and Tempel, B.L. (1994). Localization of Kv1.1 and Kv1.2, two K channel proteins, to synaptic terminals, somata, and dendrites in the mouse brain. *J Neurosci* *14*, 4588-4599. 10.1523/JNEUROSCI.14-08-04588.1994.
- Westphal, M., Jungbluth, A., Heidecker, M., Muhlbauer, B., Heizer, C., Schwartz, J.M., Marriott, G., and Gerisch, G. (1997). Microfilament dynamics during cell movement and chemotaxis

- monitored using a GFP-actin fusion protein. *Curr Biol* 7, 176-183. 10.1016/s0960-9822(97)70088-5.
- Whitaker, B.D., and Poff, K.L. (1980). Thermal adaptation of thermosensing and negative chemotaxis in *Dictyostelium*. *Exp Cell Res* 128, 87-93. 10.1016/0014-4827(80)90390-0.
- Xu, S., Offer, G., Gu, J., White, H.D., and Yu, L.C. (2003). Temperature and ligand dependence of conformation and helical order in myosin filaments. *Biochemistry* 42, 390-401. 10.1021/bi026085t.
- Yuen, I.S., Jain, R., Bishop, J.D., Lindsey, D.F., Deery, W.J., Van Haastert, P.J., and Gomer, R.H. (1995). A density-sensing factor regulates signal transduction in *Dictyostelium*. *J Cell Biol* 129, 1251-1262. 10.1083/jcb.129.5.1251.
- Zhao, M. (2009a). Electrical fields in wound healing-An overriding signal that directs cell migration. *Semin Cell Dev Biol* 20, 674-682. 10.1016/j.semcdb.2008.12.009.
- Zhao, M., Agius-Fernandez, A., Forrester, J.V., McCaig, C.D.J.I.o., and science, v. (1996). Directed migration of corneal epithelial sheets in physiological electric fields. 37, 2548-2558.
- Zhao, M., Jin, T., McCaig, C.D., Forrester, J.V., and Devreotes, P.N. (2002). Genetic analysis of the role of G protein-coupled receptor signaling in electrotaxis. *J Cell Biol* 157, 921-927. 10.1083/jcb.200112070.
- Zhao, M., Song, B., Pu, J., Wada, T., Reid, B., Tai, G.P., Wang, F., Guo, A.H., Walczysko, P., Gu, Y., et al. (2006). Electrical signals control wound healing through phosphatidylinositol-3-OH kinase- γ and PTEN. *Nature* 442, 457-460. 10.1038/nature04925.